Chemical Characterization of Organosulfates in Secondary Organic Aerosol Derived from the Photooxidation of Alkanes

M. Riva[1], T. Da Silva Barbosa[2,3], Y.-H. Lin[1,a], E. A. Stone[4], A. Gold[1], and J. D. Surratt[1,*]

[1]Department of Environmental Sciences and Engineering, Gillings School of Global Public Health, The University of North Carolina at Chapel Hill, Chapel Hill, NC, USA

[2] CAPES Foundation, Brazil Ministry of Education, Brasilia, DF 70.040-020, Brazil

[3]Departamento de Química, Instituto de Ciências Exatas, Universidade Federal Rural do Rio de Janeiro, Seropédica, Brazil

[4]Department of Chemistry, University of Iowa, Iowa City, IA 52242, United States

[a] now at: Michigan Society of Fellows, Department of Chemistry, University of Michigan, Ann Arbor, MI, USA

* To whom correspondence should be addressed.

Jason D. Surratt, Department of Environmental Sciences and Engineering, Gillings School of Global Public Health, University of North Carolina at Chapel Hill, Chapel Hill, NC 27599 USA. Tel: 1-(919)-966-0470; Fax: (919)-966-7911; Email: surratt@unc.edu

The authors declare no conflict of interest.

Abstract

We report the formation of aliphatic organosulfates (OSs) in secondary organic aerosol (SOA) from the photooxidation of C_{10} – C_{12} alkanes. The results complement those from our laboratories reporting the formation of OSs and sulfonates from gas-phase oxidation of polycyclic aromatic hydrocarbons (PAHs). Both studies strongly support the formation of OSs from the gas-phase oxidation of anthropogenic precursors, as hypothesized on the basis of recent field studies in which aromatic and aliphatic OSs were detected in fine aerosol collected from several major urban locations. In this study, dodecane, cyclodecane and decalin, considered to be important SOA precursors in urban areas, were photochemically oxidized in an outdoor smog chamber in the presence of either non-acidified or acidified ammonium sulfate seed aerosol. Effects of acidity and relative humidity on OS formation were examined. Aerosols collected from all experiments were characterized by ultra performance liquid chromatography coupled to electrospray ionization high-resolution quadrupole time-of-flight mass spectrometry (UPLC/ESI-HR-QTOFMS). Most of the OSs identified could be explained by formation of gaseous epoxide precursors with subsequent acid-catalyzed reactive uptake onto sulfate aerosol and/or heterogeneous reactions of hydroperoxides. The OSs identified here were also observed and quantified in fine urban aerosol samples collected in Lahore, Pakistan, and Pasadena, CA, USA. Several OSs identified from the photooxidation of decalin and cyclodecane are isobars of known monoterpene organosulfates, and thus care must be taken in the analysis of alkane-derived organosulfates in urban aerosol.

47

48 1. Introduction

49 Atmospheric fine aerosol ($PM_{2.5}$, aerosol with aerodynamic diameter $\leq 2.5\ \mu m$) plays a
50 major role in scattering and absorption of solar radiation, which impacts global climate (Kroll
51 and Seinfeld, 2008; Stevens and Boucher, 2012). $PM_{2.5}$ also participates in heterogeneous
52 chemical reactions, affecting the abundance and distribution of atmospheric trace gases
53 (Hallquist et al., 2009). Human exposure to $PM_{2.5}$ is associated with respiratory and
54 cardiovascular diseases (Elder and Oberdorster, 2006).

55 Typically, the largest mass fraction of $PM_{2.5}$ is organic, dominated by secondary
56 organic aerosol (SOA) formed by the oxidation of volatile organic compounds (VOCs).
57 Although SOA contributes a large fraction (20–90%, depending on location) of total $PM_{2.5}$
58 mass, current models predict less SOA than is generally observed during field measurements
59 (Kroll and Seinfeld, 2008; Hallquist et al., 2009). The omission of intermediate volatility
60 organic compounds (IVOC) as SOA precursors, such as alkanes or polycyclic aromatic
61 hydrocarbons (PAHs), could contribute in part to the underestimation of SOA mass observed
62 in urban areas (Robinson et al., 2007; Tkacik et al., 2012). Long-chain alkanes are important
63 anthropogenic pollutants emitted by combustion and vehicular sources representing up to
64 90% of the anthropogenic emissions in certain urban areas (Fraser et al., 1997, Gentner et al.,
65 2012). In the atmosphere, they are rapidly depleted by reaction with OH and NO_3 radicals
66 (Atkinson, 2000) yielding a large variety of oxygenated compounds (Lim and Ziemann, 2005;
67 2009; Yee et al., 2012; 2013), which could lead to SOA formation (Lim and Ziemman, 2009;
68 Loza et al., 2014). SOA yields have been measured for C_7-C_{25} alkanes having linear, branched
69 and cyclic structures (Lim and Ziemman, 2009; Presto et al., 2010; Tkacik et al., 2012; Loza
70 et al., 2014; Hunter et al., 2014). Structure plays a key role in SOA yield, which increases
71 with carbon number or the presence of cyclic features and tends to decrease with branching as

gas-phase fragmentation predominates (Lambe et al., 2012; Carrasquillo et al., 2014; Loza et al., 2014; Hunter et al., 2014).

The presence of organosulfates (OSs) has been demonstrated in several atmospheric compartments, including atmospheric aerosol (Iinuma et al., 2007; Gómez-González et al., 2008; Hawkins et al., 2010; Hatch et al., 2011; Kristensen et al., 2011; Stone et al., 2012; Shalamzari et al., 2013; Hansen et al., 2014; Liao et al., 2015), rain (Altieri et al., 2009), clouds and fog (Pratt et al., 2013; Boone et al., 2015), and several studies indicate that OSs could contribute to a substantial fraction (up to 30%) of the organic mass measured in ambient $PM_{2.5}$ (Surratt et al., 2008; Tolocka and Turpin, 2012).

Although the variety of OSs identified from field measurements is quite large (Surratt et al., 2008; Tao et al., 2014; Wang et al., 2015; Kuang et al., 2016), only a few OS precursors have been unequivocally identified through laboratory studies. OSs have been generated in SOA in smog chambers from OH, NO_3 or O_3 oxidation of BVOCs, including isoprene (Surratt et al., 2007; Ng et al., 2008), 2-methyl-3-buten-2-ol (MBO) (Zhang et al., 2012; Mael et al., 2015), unsaturated aldehydes (Schindelka et al., 2013; Shalamzari et al., 2014; Shalamzari et al., 2015), monoterpenes (Iinuma et al., 2007; Iinuma et al., 2009; Surratt et al., 2008), and sesquiterpenes (Liggio et al., 2006; Surratt et al., 2008; Iinuma et al., 2009; Noziere et al., 2010; Chan et al., 2011) in the presence of acidified sulfate aerosol. However, the large number of unidentified OSs having C_2 to C_{25} skeletons observed in recent field studies are clearly not derived from BVOC precursors, and suggest alkanes and aromatics as a major source of hitherto unrecognized of OS precursors (Tao et al., 2014; Wang et al., 2015; Kuang et al., 2016). Ma et al. (2014) have recently shown that the contribution of aromatic OSs could represent up to two-thirds of the OSs identified in Shanghai. Aliphatic OSs were identified in the ambient samples from urban locations (Tao et al., 2014; Wang et al., 2015; Kuang et al., 2016), suggesting that gas-phase oxidation of long-chain or cyclic alkanes could be an

97 important source of OSs (Tao et al., 2014). At present, lack of authentic standards prevents
98 quantitation of the OSs contribution to $PM_{2.5}$ mass, underscoring the need to better identify the
99 OS precursors.

100 Studies on the impact of NO_x and O_3 on SOA formation from oxidation of long-chain
101 alkanes (Loza et al., 2014; Zhang et al., 2014) have shown that the presence of NO_x tends to
102 reduce SOA formation by reaction of peroxy radicals (RO_2) with NO, to yield alkoxy radicals
103 (RO). For alkanes containing fewer than 10 carbons, the fragmentation/decomposition of RO
104 radicals will produce higher volatility species (e.g., small carbonyls), which suppresses or
105 reduces SOA formation (Lim and Ziemann, 2005, 2009). Recent studies have shown that
106 increased aerosol acidity is a key variable in enhancing SOA formation through acid-
107 catalyzed reactive uptake and multiphase chemistry of oxidation products derived from
108 biogenic VOCs (BVOCs) such as isoprene (Surratt et al., 2010) and α-pinene (Iinuma et al.,
109 2009). Formation of highly oxidized products, including OSs, demonstrates the importance of
110 heterogeneous processes, such as reactive uptake of epoxides onto acidic sulfate aerosol, in
111 SOA formation (Iinuma et al., 2009; Surratt et al., 2010; Chan et al., 2011; Lin et al., 2014;
112 Shalamzari et al., 2015). OSs may also be formed by either nucleophilic substitution of
113 organic nitrates by sulfate (Darer et al., 2011; Hu et al., 2011) or by heterogeneous oxidation
114 of unsaturated compounds involving sulfate anion radicals (Noziere et al., 2010; Schindelka et
115 al., 2013; Schone et al., 2014).

116 Formation of OSs from the gas-phase oxidation of the C_{10} alkanes, cyclodecane
117 ($C_{10}H_{20}$) and decalin (bicyclo[4.4.0]decane; $C_{10}H_{18}$), and C_{12} alkane, dodecane ($C_{12}H_{26}$), in the
118 presence of sulfate aerosol under varying acidities is reported in this work. These alkanes
119 were selected based on their potential contribution to atmospheric SOA formation (Hunter et
120 al., 2014). Studies have demonstrated that cyclic compounds ($< C_{12}$) are expected to be more
121 efficient SOA precursors than linear or branched alkanes with the same number of carbons

(Lim and Ziemann, 2005; Pye and Pauliot, 2012). Alkanes ≥ C_{10} are considered as effective SOA precursors, especially when placed in the context of their emission rates (Pye and Pauliot, 2012). Effects of RH and aerosol acidity on OS formation were investigated. SOA collected from outdoor smog chamber experiments was chemically characterized by ultra performance liquid chromatography interfaced to high-resolution quadrupole time-of-flight mass spectrometry equipped with electrospray ionization (UPLC/ESI-HR-QTOFMS). In addition, effect of solvent mixture (methanol vs acetonitrile/toluene) on OS quantification was investigated. Finally, $PM_{2.5}$ samples collected from Lahore, Pakistan and Pasadena, CA, USA were analyzed to detect and quantify OSs identified from the smog chamber experiments.

2. Experimental

2.1 Chamber Experiments. Eighteen experiments were performed at the University of North Carolina (UNC) outdoor smog chamber facility located at Pittsboro, NC. Details of this facility have been previously described (Lee et al., 2004; Kamens et al., 2011). Briefly, it is a 274–m^3 dual chamber divided into two sides by a Teflon film curtain. One side referred as "North Chamber" has an actual volume of 136 m^3, and the other side referred as "South Chamber" has an actual volume of 138 m^3. Prior to each experiment, both sides of the chamber were flushed using rural background air using an exhaust blower for at least 12 hours. Clean air was then injected into both sides of the chamber using a clean air generator to reduce concentrations of background aerosol and VOCs. Experiments were performed under two humidity conditions: at low RH (10–20%) and high RH (40–60%). For experiments conducted at low RH (i.e., dry), the clean air generator was used after the preliminary venting using rural air for approximately 48–72 hours. A scanning mobility particle sizer (SMPS, TSI 3080) was used to measure aerosol size distributions, including number and volume concentrations inside both chambers. Before each experiment, the typical aerosol mass

147 concentration (assuming an aerosol density of 1 g cm^{-3}) background was less than ~ 3 μg m^{-3}
148 in humid conditions and less than ~ 0.2 μg m^{-3} for dry experiments. Either non-acidified or
149 acidified ammonium sulfate seed aerosols were introduced into the chambers by atomizing
150 aqueous solutions of 0.06 M $(NH_4)_2SO_4$ or 0.06 M $(NH_4)_2SO_4$ + 0.06 M H_2SO_4, respectively.
151 After 15 min of atomization, ~ 40 μg m^{-3} of seed aerosol was injected into the chambers.
152 After stabilization of aerosol volume concentrations, Teflon blank filters were collected (47
153 mm diameter, 1.0 μm pore size, Tisch Environmental, EPA $PM_{2.5}$ membrane) over 45 min at
154 a sampling rate of ~ 25 L min^{-1} in order to measure baseline aerosol composition prior to
155 injection of the SOA precursors. None of the aliphatic OSs produced from the oxidation of
156 studied alkanes were detected in the chamber background. Dodecane (Sigma-Aldrich, 99%),
157 cyclodecane (TCI, 94%) or decalin (Sigma-Aldrich, 99%, mixture of *cis* + *trans*) were
158 introduced into both sides of the chamber by passing a N_2 flow through a heated manifold
159 containing a known amount of liquid compound. Concentrations of alkanes were measured
160 online in each side every 10 minutes by a gas chromatograph with a flame ionization detector
161 (GC–FID, Model CP-3800, Varian), calibrated before each experiment with a standard
162 mixture of hydrocarbons. Isopropyl nitrite (IPN) (Pfaltz & Bauer, 97%) was used as an OH
163 radical source (Raff and Finlayson-Pitts, 2010) and was injected into both sides when VOC
164 signals were stable as measured by the GC–FID. O_3 and NO_x concentrations were monitored
165 using UV photometric and chemiluminescent analyzers, respectively (O_3: Model 49P,
166 Thermo-Environmental; NO_x: Model 8101B, Bendix). Both instruments were calibrated as
167 described in previous work (Kamens et al., 2011). Dilution rate for each chamber was
168 monitored by sulfur hexafluoride (SF_6) measured using gas chromatography with electron
169 capture detection (GC–ECD). RH, temperature, irradiance and concentration of O_3 and NO_x
170 were recorded every minute. SOA formation from alkane photooxidation was monitored for
171 all experiments. 2–3 hours following IPN injection, which corresponds to the end of SOA

growth as measured by the SMPS, filter sampling was initiated. For each experiment, two filters from each side of the chamber were collected for 45 min – 2 hours (sampling rate ~ 25 L min^{-1}) to characterize particle-phase reaction products. Based on SOA volume concentrations measured by the SMPS, sampling time was adjusted to obtain an SOA mass of about ~ 100 μ g/filter. Experimental conditions are summarized in Table 1.

2.2 Ambient Aerosol Collection. Five filters collected in Lahore (Pakistan) between January 2007 and January 2008 (Stone et al., 2010) and eight filters collected in Pasadena CA, (USA) during the 2010 California Research at the Nexus of Air Quality and Climate Change (CalNex) field study from 15 May − 15 June 2010 (Hayes et al., 2013), were analyzed for the OSs identified in smog chamber experiments. $PM_{2.5}$ was collected on prebaked quartz fiber filters (QFF, Pall Life Sciences, Tissuquartz, 47 mm for Lahore, 20.3 cm × 25.4 cm for Pasadena) using a medium-volume sampling apparatus at Lahore (URG-3000, Chapel Hill, NC, USA) and a high-volume sampler (Tisch Environmental, Cleves, OH, USA) at Pasadena. As stipulated previously at both urban sites, anthropogenic activities (e.g., vehicular exhaust, industrial sources, cooking, etc.) likely dominated the organic aerosol mass fraction of $PM_{2.5}$ (Stone et al., 2010; Hayes et al., 2013). In addition, Gentner et al. (2012) have reported significant emission of long-chain alkanes during the CalNex field study.

2.3 Filter Extraction. The impact of the solvent mixture on OS quantification was also explored in this work. Filters collected from smog chamber experiments were extracted using two different solvent mixtures. One filter was extracted using 22 mL of high-purity methanol (LC-MS CHROMASOLV-grade, Sigma-Aldrich, ≥ 99.9 %) under 45 min (25 min + 20 min) of sonication at room temperature while the second filter was extracted using 22 mL of a 70/30 (v/v) solvent mixture containing acetonitrile/toluene (CHROMASOLV-grade, for HPLC, Sigma-Aldrich, ≥ 99.9 %). Extracts were then blown dry under a gentle nitrogen stream at ambient temperature (Surratt et al., 2008; Zhang et al., 2011; Lin et al., 2012). Dry

extracts were then reconstituted with 150 μL of either a 50:50 (v/v) solvent mixture of methanol and water (MilliQ water) or a 50:50 (v/v) solvent mixture of acetonitrile and water. Filters collected from field studies were extracted using methanol as solvent and following the protocol described above; however, prior to drying, extracts were filtered through 0.2-μm PTFE syringe filters (Pall Life Science, Acrodisc) to remove insoluble particles or quartz filter fibers.

2.4 Chemical Analysis. Characterization of OSs in chamber experiments was performed using ultra performance liquid chromatography interfaced to a high-resolution quadrupole time-of-light mass spectrometer equipped with an electrospray ionization source (UPLC/ESI-HR-Q-TOFMS, 6500 Series, Agilent) operated in the negative ion mode. Exact operating conditions have been previously described (Lin et al., 2012). 5 μL sample aliquots were injected onto a UPLC column (Waters ACQUITY UPLC HSS T3 column). Octyl sulfate ($C_8H_{17}O_4S^-$; Sigma-Aldrich) and 3-pinanol-2-hydrogen sulfate ($C_9H_{13}O_6S^-$) were used as surrogate standards to quantify the identified aliphatic OSs.

2.5 Total Organic Peroxide Analysis. The total organic peroxides in the SOA were quantified using an iodometric-spectrophotometric method adapted from Docherty et al. (2005). As described in Surratt et al. (2006), the method employed in this work differs in the choice of extraction solvent: we used a 50:50 (v/v) mixture of methanol and ethyl acetate, rather than pure ethyl acetate. Calibrations and measurements were performed at 470 nm using a Hitachi U-3300 dual beam spectrophotometer. Benzoyl peroxide was used as the standard for quantification of organic peroxides formed from alkane oxidations. The molar absorptivity measured from the calibration curve was ~ 825, which is in excellent agreement with previously reported values (Docherty et al., 2005; Surratt et al., 2006).

3. Results and Discussion

In the subsequent sections, detailed chemical characterization of OSs identified from the gas-phase oxidation of dodecane, decalin and cyclodecane in the presence of ammonium sulfate aerosol is presented. The presence of OSs was revealed by the appearance of characteristic fragment ions at *m/z* 79.95 ($SO_3^{\bullet/-}$), 80.96 (HSO_3^-) and/or 96.96 (HSO_4^-) in tandem mass spectra (MS^2) (Iinuma et al., 2007; Gómez-González et al., 2008; Surratt et al., 2008; Shalamzari et al., 2013; 2014). Tentative structures, retention times and exact mass measurements of OSs detected in this work are reported in Table S1. The low abundance of some OSs precluded acquisition of high-resolution MS^2 data and thus structures have not been proposed for the low-abundance parent ions.

3.1 Characterization of OSs from Dodecane Photooxidation. Seven OSs, including isobaric compounds, were identified in SOA produced from the gas-phase oxidation of dodecane in the presence of sulfate seed aerosol. None have previously been reported in chamber experiments, although they have recently been observed in ambient fine aerosol samples (Tao et al., 2014; Kuang et al., 2016). Concentrations of the products are reported in Table S2. Three isobaric parent ions with *m/z* 279 ($C_{12}H_{23}O_5S^-$, 279.1254), hereafter referred to as OS-279, were identified in SOA generated from dodecane oxidation in the presence of acidified ammonium sulfate aerosol. Kwok and Atkinson (1995) have reported that OH oxidation of long-chain alkane preferentially occurred at an internal carbon and thus multiple isomers may be proposed. Based on Yee et al. (2012; 2013) one isomer may be, however, assigned as 6-dodecanone-4-sulfate. The MS^2 spectra of the products were identical, having product ions diagnostic for a sulfate ester β to an abstractable proton (Surratt et al., 2008; Gómez-González et al., 2008) at *m*/z 199 ($C_{12}H_{23}O_2^-$, loss of neutral SO_3) and 97 (HSO_4^-), precluding assignment of positional isomerism. Figures 1 and S1 present the MS^2 spectrum of OS-279 and proposed fragmentation pathway, respectively. By chemical ionization mass

247 spectrometry (CIMS) operating in the negative mode, Yee et al. (2012) identified the
248 formation of hydroperoxides from the oxidation of dodecane under low–NO_x conditions,
249 confirming the predicted RO_2 – HO_2 reaction pathway in the low–NO_x regime. First-
250 generation hydroperoxides ($C_{12}H_{26}O_2$) can undergo further oxidation by reaction with OH to
251 form either more highly oxidized products, such as dihydroperoxides ($C_{12}H_{26}O_4$), or semi-
252 volatile products ($C_{12}H_{24}O$) (Yee et al., 2012). In addition, hydroperoxides can be photolyzed
253 to alkoxy radicals (RO) to form more highly oxidized products. Low-volatility products could
254 then condense onto sulfate aerosols and undergo further heterogeneous reactions (Schilling
255 Fahnestock et al., 2015) leading to OSs as discussed below. In our study, OH radicals were
256 formed from IPN photolysis without additional injection of NO. Under these conditions, RO_2
257 chemistry is dominated by RO_2 + HO_2 and/or RO_2 + RO_2 reactions as discussed by Raff and
258 Finlayson-Pitts (2010). Although RO_2 radicals could also react with NO formed by either IPN
259 or NO_2 photolysis, formation of ozone under chamber conditions (0.3-0.6 ppm, depending on
260 the concentration of IPN injected, Table 1) would rapidly quench NO (Atkinson et al., 2000).
261 Therefore, RO_2 + NO reactions are not expected to be significant. In addition, total organic
262 peroxide aerosol concentrations, presented in Table 1, reveal that organic peroxides account
263 (on average) for 28 % of the SOA mass measured in the different experiments in support of a
264 significant contribution of RO_2 + RO_2/HO_2 and/or RO_2 autoxidation to SOA formation from
265 alkane oxidations.

266 Carbonyl hydroperoxide ($C_{12}H_{24}O_3$), which has been identified in the gas phase by Yee
267 et al. (2012), is likely involved in acid-catalyzed heterogeneous reactions onto sulfate aerosol.
268 Heterogeneous chemistry of gas-phase organic peroxides has been previously suggested to
269 explain the formation of certain OSs and tetrols (Riva et al., 2016). Acid-catalyzed
270 perhydrolysis of hydroperoxides followed by reaction with sulfate anion radicals could also
271 be possible route to the formation of OS-279 (Figure 1). However, further investigation is

required to better understand how acidified sulfate seed aerosol takes up organic peroxides from the gas phase and how particle-phase reactions might degrade organic peroxides into OSs. It should be mentioned that photooxidation of dodecane has also been investigated using an additional injection of NO (200 ppb) prior IPN injection. In this experiment SOA formation was significantly reduced as well as the OS concentrations (factor of 3-4), confirming that NO strongly impacts the formation of OSs, such as OS-279.

3.2 Characterization of OSs from Decalin Photooxidation. Gas-phase oxidation of cyclic alkanes at room temperature and atmospheric pressure has received less attention than linear or branched alkanes. However, recent studies have demonstrated that oxidations of cyclic alkanes by OH radicals produce less−volatile oxygenated compounds and have larger SOA yields (Lim and Ziemann, 2005; Lambe et al., 2012; Tkacik et al., 2012; Yee et al., 2013; Hunter et al., 2014; Loza et al., 2014). Significant formation of OSs (up to 1 μg m^{-3}) and SOA were observed in all experiments of decalin photooxidation (Tables 1 and S3), revealing the high potential for bicyclic alkanes to form OSs. All OSs (25 OSs including isomeric/isobaric structures) identified from the oxidation of decalin in the presence of ammonium sulfate aerosol have been observed in ambient aerosol, underscoring the potential importance of alkanes to OS formation in urban areas (Tao et al., 2014; Wang et al., 2015; Kuang et al., 2016). MS^2 spectra were obtained for all OSs identified from decalin oxidation, except for parent ions at *m/z* 195.0697 (OS-195) and 299.0805 (OS-299). All of the parent ions show an intense product ion at *m/z* 96.96, indicative of an aliphatic sulfate ester. Retention times and tentative structural assignments are given in Table S1.

Figures 2 and S2 present MS^2 spectra and fragmentation schemes of selected parent ions at *m/z* 265.0752 (OS-265), 269.0696 (OS-269), 295.0494 (OS-295) and 326.0554 (OS-326). MS^2 spectra and fragmentation schemes of other OSs are reported in Figure S3-S7. These selected OSs exhibit specific fragmentation patterns and were, as described in the next

297 section, quantified and characterized in the fine urban aerosol samples. The different reaction
298 pathways presented below, are separated based on OSs that are generated from branching
299 reactions of a common transient. Four isomers of OS-265 with composition $C_{10}H_{17}O_6S^-$ were
300 identified in decalin-derived SOA collected from all experiments. With regard to components
301 of ambient SOA, it is important to mention that the formation of isobaric OSs with the same
302 elemental composition of $C_{10}H_{17}O_6S^-$ isobars have also been previously identified in SOA
303 produced from the gas-phase oxidation of monoterpenes (Liggio et al., 2006; Surratt et al.,
304 2008) and are not unique to decalin oxidation. The product ion at nominal *m/z* 97 (HSO_4^-) and
305 loss of neutral SO_3 in the MS^2 spectrum (Figure 2a) is consistent with an aliphatic OS having
306 a labile proton in a β position (Attygalle et al., 2001). Absence of product ions corresponding
307 to a loss of a terminal carbonyl (–CO) or a carboxyl group ($–CO_2$), respectively (Romero and
308 Oehme, 2005; Shalamzari et al., 2014), and a composition corresponding to 2 double bond
309 equivalencies (DBEs) has thus been attributed to an internal carbonyl group and a six-
310 membered ring. A scheme leading to the structure proposed in Figure 2a is based on the
311 cleavage of the C_1–C_2 decalin bond, followed by reaction with a second O_2 molecule and HO_2
312 leads to a terminal carbonyl hydroperoxide ($C_{10}H_{18}O_3$) (Yee et al., 2013). $C_{10}H_{18}O_3$ could then
313 further react with OH radicals and lead to an epoxide and sulfate ester by reactive
314 uptake/heterogeneous chemistry (Paulot et al., 2009). OS-265 ($C_{10}H_{17}O_6S^-$) could also arise
315 from the acid-catalyzed perhydrolysis of the hydroperoxide ($C_{10}H_{18}O_4$) generated from the
316 reaction of $C_{10}H_{17}O_4^{\bullet}$ + HO_2 (Figure S8, pathway b). The MS^2 spectrum for the single parent
317 ion at *m/z* 281 corresponding to the composition $C_{10}H_{17}O_7S^-$ (OS-281) gave product ions
318 expected for a sulfate ester β to a labile proton with 2 DBE, but no additional structural
319 information (Figure S4). The pathway proposed in Figure S8 pathway **b** is based on gas-phase
320 oxidation of a 4-(cyclohexan-2-one)but-1-yl radical followed by reaction with O_2 and a 1,5-H
321 shift (Crounse et al., 2011; Orlando and Tyndall, 2012) and lead to a C_{10}-carbonyl-

hydroxyhydroperoxide ($C_{10}H_{18}O_4$). $C_{10}H_{18}O_4$ could then further react with OH radical and by elimination of OH lead to an epoxide (Figure S8, pathway **b**). In addition, OS-281 could arise from acid-catalyzed perhydrolysis of C_{10}-carbonyl dihydroperoxides ($C_{10}H_{18}O_5$) as proposed in Figure S8, pathway **c**. The direction of ring opening of the internal epoxide by reactive uptake to give the final product is arbitrary. Three isobaric parent ions at *m/z* 297 corresponding to the composition $C_{10}H_{17}O_8S^-$ with 2 DBEs were identified. Loss of water, HSO_4^- and SO_3 as a neutral fragment in the MS^2 spectrum of the major isobar (OS-297) is consistent with a hydroxyl-substituted sulfate ester β to a labile proton (Figure S6). The scheme proposed in Figure S8 pathway **c** is based on the oxidation to a 4-(cyclohexan-2-one)but-1-yl radical as in pathway **b**. However, in contrast to pathway **b**, RO_2 formed by the addition of O_2 undergoes a 1,6-H shift (Crounse et al., 2011; Orlando and Tyndall, 2012) followed by addition of a second O_2 molecule, a 1,5-H shift and elimination of OH to yield an epoxide, which leads to a sulfate ester by reactive uptake onto acidified aerosols. The direction of ring opening of the internal alkyl epoxide is arbitrary.

The composition of the parent ion at *m/z* 269.0696 ($C_9H_{17}O_7S^-$) corresponds to one DBE. MS^2 spectrum yields products consistent with a sulfate ester β to an abstractable proton and similar to OS-265, neither a terminal carbonyl nor a carboxyl functional group was detected in the OS-269. As a result, the presence of hydroperoxide and/or hydroxyl substituents is expected in order to satisfy the molecular formulas obtained by the accurate mass measurement. Although ESI-MS in the negative ion mode is not sensitive to multifunctional hydroperoxides and alcohols (Cech and Enke, 2001; Witkowski and Gierczak, 2012), this technique is highly sensitive to hydroperoxides and alcohols, which also contain OS groups and give $[M - H]^-$ ions (Surratt et al., 2008; Kristensen et al., 2011; Kundu et al., 2013; Hansen et al., 2014).

346 In Figure 3, tentative pathways leading to the formation of OS-267, OS-269 and OS-
347 285 are proposed. Under low-NO_x conditions, abstraction of a proton α to the ring scission of
348 decalin followed by reaction with O_2 leads to the 1-hydroperoxy radical, which in turn can
349 react with another RO_2 radical to yield the corresponding alkoxyl radical ($C_{10}H_{17}O^{\bullet}$)
350 (Atkinson, 2000). Cleavage of the C_1–C_2 decalin bond, followed by reaction with a second O_2
351 molecule and HO_2 leads to a terminal carbonyl hydroperoxide ($C_{10}H_{18}O_3$) (Yee et al., 2013).
352 The aldehydic intermediate in the sequence following C_1-C_2 ring scission may be oxidized to
353 the corresponding acyl radical either by photolysis (Wang et al., 2006) or by H-abstraction
354 (Kwok and Atkinson 1995) followed by addition of O_2, reaction with RO_2 or HO_2 and
355 decarboxylation of the resulting acyl-oxy radical (R(O)O) (Chacon-Madrid et al., 2013) to a
356 hydroperoxyperoxy radical ($C_9H_{17}O_4^{\bullet}$). $C_9H_{17}O_4^{\bullet}$ can react via pathway **a** (Figure 3) through a
357 1,6-H shift (Crounse et al., 2011; Orlando and Tyndall, 2012) followed by elimination of OH
358 resulting in a formation of an epoxide analogous to the formation of isoprene epoxydiol
359 (IEPOX) (Paulot et al., 2009; Mael et al., 2015). The epoxide can then undergo acid-catalyzed
360 ring opening to give OS-269 ($C_9H_{17}O_7S^-$). The MS^2 spectrum of OS-285 ($C_9H_{17}O_8S^-$; Figure
361 S5) shows product ions corresponding to HSO_3^-, HSO_4^- and loss of neutral SO_3, in accord
362 with a sulfate ester β to a labile proton, but yields no further structural information. The
363 structure proposed for OS-285 is based on the formation of reaction of the
364 hydroperoxyperoxyl radical intermediate in pathway **b** with RO_2 followed by a 1,4-H shift
365 (Rissanen et al., 2015) and addition of O_2 to give a hydroxyhydroperoxyperoxyl radical
366 ($C_9H_{17}O_5^{\bullet}$). $C_9H_{17}O_5^{\bullet}$ could then lead to an epoxide by isomerization (Iinuma et al., 2009;
367 Surratt et al., 2010; Jacobs et al., 2013; Mael et al., 2015) and form OS-285. $C_9H_{17}O_5^{\bullet}$ could
368 also react with HO_2 and form the corresponding C_9-hydroxydihydroperoxide ($C_9H_{18}O_5$), which
369 could then undergo heterogeneous reaction and lead to OS-269 (Figure 3, pathway **b**). Finally,
370 a C_9-carbonyl hydroperoxide ($C_9H_{16}O_3$) could also be formed from the RO + O_2 reaction

371 (Figure 3, pathway **c**), which could then further react with OH radicals and lead to a C_9-
372 carbonyl dihydroperoxide ($C_9H_{16}O_5$). Hence, $C_9H_{16}O_5$ could form OS-267 ($C_9H_{15}O_7S^-$) from
373 heterogeneous reaction on acidic aerosols.

374 In Figure 4, pathways from an initial 1-peroxy transient are proposed to products
375 designated OS-295, OS-311 and OS-326. Three isobaric ions corresponding to OS-295
376 ($C_{10}H_{15}O_8S^-$) were identified in decalin-derived SOA under all experimental conditions.
377 Figure 2c shows the MS^2 spectrum of the parent ion at *m/z* 295. A product ion at *m/z* 251
378 corresponding to loss of CO_2 (Romero and Oehme, 2005; Shalamzari et al., 2014) is present
379 in addition to product ions consistent with a sulfate ester β to a labile H (Riva et al., 2015).
380 Pathway **a** leads to the structure consistent with the MS^2 spectrum and 3 DBEs required by
381 the composition of the parent ion. The salient features of pathway **a** include oxidation of the
382 RO_2 to 2-decalinone, formation of a C_{10} alkoxy radical followed by ring cleavage of the
383 C_9–C_{10} decalin bond and further RO_2 isomerization (1,8-H shift) leading to a 4-(carboxy
384 cyclohexyl)-1-hydroperoxybut-2-yl radical via RO_2 chemistry. Although considered as a
385 minor reaction pathway (Crounse et al., 2013), the acyloxy radical could lead to the epoxide
386 from the isomerization of the O_2 adduct (Paulot et al., 2009; Yao et al., 2014; Zhang et al.,
387 2015). Further acid-catalyzed ring opening of the epoxide leads to OS-295 ($C_{10}H_{15}O_8S^-$).

388 Two isobaric parent ions with identical MS^2 spectra were observed at *m/z* 311
389 ($C_{10}H_{15}O_9S^-$; Figure S7). The only observed product ion at *m/z* 97 is consistent with a sulfate
390 ester, but not informative with regard to a more refined assignment of molecular structure.
391 Pathway **b** to a hydroperoxide for the parent ion with 3 DBEs is proposed by analogy to the
392 putative hydroperoxide structures of OS-267, OS-269 and OS-285. Pathway **b** is
393 characterized by a H-abstraction from a carbon at the ring fusion of 2-decalinone leading to
394 formation of an 2-decalinone-6-oxy radical followed by a sequence of ring cleavage, O_2
395 additions and H-shifts to form a 4-(2,6-cyclohexyl)-2-hydroperoxybutan-1-oxide that can

form the sulfate ester on reactive uptake. Abstraction of H1 rather than H6 would lead to an isobaric structure.

Four isobaric ions corresponding to $C_{10}H_{16}NO_9S^-$ with analogous MS^2 spectra (Figure 2d) were detected at nominal mass *m/z* 326. The loss of 63 mass units as neutral HNO_3 (Figure S2d) is in accord with a nitrate ester (Surratt et al., 2008), supported by the absence of product ions from loss of NO or NO_2 (Kitanovski et al., 2012). Although RO_2 + NO reactions are expected to be minor under the conditions used in this work (i.e. NO < 1 ppb, formation of RO radicals or organonitrates cannot be ruled out. Indeed, Ehn et al. (2014) have demonstrated that NO reactions could be competitive at ppb levels. Under our experimental conditions RO_2 + NO, RO_2 + HO_2/RO_2 and RO_2 autoxidation are possible. Therefore, the parent ion at *m/z* 326 could arise from the reaction of the decalin-2-peroxy radical with NO to form decalin-2-nitrate ($C_{10}H_{17}NO_3$) with subsequent reactions shown in Figure 4, pathway **c**. From this point, a sequence of reactions identical to pathway **b** yields the parent OS-326. It is important to mention that the formation of isobaric OSs with the same elemental composition of $C_{10}H_{16}NO_9S^-$ isobars have also been identified in SOA produced from the gas-phase oxidation of monoterpenes (Surratt et al., 2008).

3.3 Characterization of OSs from Cyclodecane Photooxidation. The concentrations of OSs identified from gas-phase oxidation of cyclodecane are reported in Table S4. High levels of OSs were observed in experiments performed under dry conditions with acidified ammonium sulfate seed aerosol. The impact of acidity on OS formation will be discussed in more detail in the following section. The MS^2 spectra of all cyclodecane products show only a single product ion at nominal *m/z* 97 corresponding to bisulfate (Figures S9 – S13), indicating that the oxidation products are sulfate esters β to a labile proton. None of the fragment ions observed in the MS^2 spectrum suggests the presence of a terminal carbonyl or a carboxyl functional group in the cyclodecane-OSs, which is consistent with conservation of the

cyclodecane ring. Tentative structures proposed in Table S1 are based on DBE calculations and retention of the cyclodecane ring supported by MS^2 data. Pathways proposed in Figure S14 are initiated by H-abstraction and based on reaction sequences for which precedent has been established: addition of O_2 to cycloalkyl radicals to give RO_2 which either reacts with RO_2 to yield alkoxy radicals (Atkinson and Arey, 2003; Ziemann and Atkinson, 2012) or undergoes intramolecular H-shifts leading to generation of hydroperoxides (Ehn et al., 2014; Jokinen et al., 2014; Mentel et al., 2015). The formation of compounds such as cyclodecanone ($C_{10}H_{18}O$), cyclodecane hydroperoxide ($C_{10}H_{20}O_2$) or cyclodecane hydroxyhydroperoxide ($C_{10}H_{20}O_3$) are proposed as intermediate products leading to epoxy-compounds after additional oxidation/isomerization processes, as presented in Figure S14. In addition $C_{10}H_{20}O_3$, cyclodecane hydroperoxide ketone ($C_{10}H_{18}O_3$) and cyclodecane hydroxyoxohydroperoxide ($C_{10}H_{18}O_4$), proposed as intermediate products, could condense onto wet acidic aerosols and lead to the corresponding OSs through acid-catalyzed perhydrolysis reactions (Figure S14). Since authentic standards are unavailable and the MS^2 data do not allow specific structural features to be assigned, the end products in pathways in Figure S14 are arbitrary. Isobars may be explained by *cis*/*trans* epoxide ring opening or the span of an H-shift (1,5-,/1,8-H shifts are possible) (Orlando and Tyndall, 2012). In the case of OS-249, where *cis*/*trans* isomers are not possible; the two isobaric structures may result from different H-shifts. OS-265 and OS-281 are reported here for the first time in chamber studies.

3.4 Impact of Relative Humidity and Acidity on OS Formation. Experiments were performed under conditions reported in Table 1. As shown in Figure 5 and Tables S2-S4, the presence of acidic aerosols significantly increases OS formation in most cases, as previously observed for OSs in SOA generated from biogenic sources (Iinuma et al., 2007; Surratt et al., 2007; Chan et al., 2011). Since differences in meteorology could impact experimental results from the outdoor chamber, caution must be exercised in comparing experiments performed on

different days. However, same-day, side-by-side experiments allow for clear resolution of the effects of aerosol acidity and seed composition on OS formation. When comparing experiments performed under dry versus wet conditions with acidified ammonium sulfate aerosol, higher RH conditions significantly reduce OS formation, likely attributable to an increase in pH because of dilution by additional particle water. To better investigate the effect of acidity on OS formation, products were divided in two groups (Figure 5), those whose concentrations were increased by a factor ≥ 2 (Group-1) and ≤ 2 (Group-2). Figure 5 and Tables S2-S4 show that OSs identified from dodecane photooxidation belong to Group-2, with the exception of OS-279. OSs from decalin photooxidation, including OS-195, OS-269 and OS-297 belong to Group-2 as well. OSs can be formed via different pathways, including acid-catalyzed ring-opening reactions of epoxy-containing SOA constituents, reactive uptake of unsaturated compounds into the particle phase, or by reaction with the sulfate anion radical (Rudzinski et al., 2009; Nozière et al., 2010; Schindelka et al., 2013; Schöne et al., 2014). OSs may also result from nucleophilic substitution of nitrate by sulfate (Darer et al., 2011; Hu et al., 2011). The impact of acidity on OS formation arising from the different pathways has been investigated principally for reactive uptake of epoxy-compounds (Jacobs et al., 2013; Lin et al., 2012; Gaston et al., 2014; Riedel et al., 2015) for which OS formation is strongly enhanced under acidic conditions (Lin et al. (2012). However, a similar enhancement was not observed in our study on PAH-OSs, which were not expected to result from epoxide chemistry (Riva et al., 2015). Based on these observations, the formation of Group-1 OSs are hypothesized to be products of reactive uptake of gas-phase epoxides.

3.5 Impact of Solvent Mixture on OS Quantification. Additional filters were collected from each side of the outdoor chamber and for each experiment to investigate the impact of solvent mixture on OS quantification. Tao et al. (2014) have recently reported that less polar solvents such as an acetonitrile (ACN)/toluene mixture are a better choice for extraction of long alkyl-

chain OSs from filters using a nanospray-desorption electrospray ionization mass spectrometry where the extraction occurs *in situ* and the analyses are qualitative. Figure 6 demonstrates that, overall, concentrations of OSs (ng m^{-3}) from the photooxidation of dodecane, decalin and cyclodecane seem to be more efficiently extracted by the ACN/toluene mixture. Tables S2-S4, showing the ratios of the concentrations individual OSs extracted by the ACN/toluene mixture divided by the concentration of OSs extracted by methanol, indicates that all $C_{10}-$ and $C_{12}-$ OS products, including highly oxidized OS, appear more efficiently extracted by the ACN/toluene mixture. For OSs smaller than C_{10}, extraction efficiencies are about the same. As noted above, isobars of OSs identified from the oxidation of alkanes have been observed in SOA generated from the oxidation of monoterpenes that are currently used as tracers for monoterpene SOA chemistry (Hansen et al., 2014; Ma et al., 2014). Hence, in addition to the caution that quantitation of alkane and monoterpene OSs is uncertain in the absence of authentic standards, some monoterpene OSs may be underestimated if not fully extracted because most studies use methanol as an extraction solvent (Surratt et al., 2008; Iinuma et al., 2009). More work is, however, needed to better characterize and elucidate the impact of solvent on the quantitation of biogenic and anthropogenic OSs, especially compounds > C_{10}.

3.6 OSs Derived from Alkanes in Ambient Fine Urban Aerosol. Archived fine urban aerosol samples collected at Lahore, Pakistan, and Pasadena, CA, USA were used to evaluate and quantify OSs identified in SOA produced from the photooxidation of alkanes. Filters were initially extracted using methanol and comparison to OSs quantified using another solvent mixture was not possible. As previously mentioned, seven parent ions have been observed in laboratory studies. Therefore, extracted ion chromatograms (EICs) obtained from smog chamber experiments were compared to those obtained from both urban locations to confirm that observed OSs correspond to OSs identified in our lab study. Figures 7 and S15

present the EICs of OSs observed in both ambient and our smog chamber-generated SOA. Table 2 identifies 12 OSs, along with concentrations, present in $PM_{2.5}$ collected from Lahore, Pakistan and Pasadena, CA, USA and also observed in our smog-chamber-generated SOA.

The high concentrations, especially at Lahore (Pakistan) of the OSs measured in the ambient aerosol samples support their use as tracers for SOA produced from the oxidation of alkanes in urban areas. This is consistent with recent proposals (Tao et al., 2014). OS-195 ($C_7H_{15}O_4S^-$), OS-249 ($C_{10}H_{17}O_5S^-$), OS-255 ($C_9H_{19}O_6S^-$), OS-267 ($C_{10}H_{19}O_6S^-$), OS-281 ($C_{10}H_{17}O_7S^-$), OS-299 ($C_{10}H_{19}O_8S^-$), OS-307 ($C_{12}H_{19}O_7S^-$) and OS-311 ($C_{10}H_{15}O_9S^-$) have been recently identified in ambient aerosol collected from the major urban locations Shanghai and Hong Kong (Tao et al., 2014; Wang et al., 2015; Kuang et al., 2016). In the absence of retention times and chromatographic conditions, OS isobars such as OS-249 or OS-279, which are currently assigned to biogenic-derived OSs (Ma et al., 2014), could also arise from anthropogenic sources such as photooxidation of cyclodecane, especially in urban areas.

4. Conclusions

The present study demonstrates the formation of OSs from the photooxidation of alkanes and complements the smog chamber study on formation of OSs and sulfonates from photooxidation of PAHs (Riva et al., 2015). Together, the results strongly support the importance of the contribution of anthropogenic precursors to OS in ambient urban $PM_{2.5}$ proposed on the basis of aromatic and aliphatic OSs in fine aerosol collected from several major urban locations (Kundu et al., 2013, Tao et al., 2014). Chemical characterization of OSs that were identified in SOA arising from the photooxidation of alkanes were performed and tentative structures have been proposed for OSs identified from the photooxidation of decalin, cyclodecane, and dodecane based on composition from exact mass measurement, DBE calculations and the transformations expected from hydroxyl radical oxidation dominated by

521 RO_2/HO_2 chemistry. Enhancement of OS yields in the presence of acidified ammonium
522 sulfate seed is consistent with reactive uptake of gas-phase epoxides as the pathway for OS
523 formation. As previously proposed for IEPOX formation (Paulot et al. 2009), isomerization of
524 RO_2 species to β hydroperoxy alkyl radicals followed by elimination of OH, is a plausible
525 pathway to gas-phase epoxides. However, more work is required to validate pathway(s)
526 leading to the formation of gaseous epoxy-products, since OS formation from other chemical
527 pathways such as nuclophilic substitution of the $–ONO_2$ group by a $–OSO_3$ group cannot be
528 ruled out (Darer et al., 2011; Hu et al., 2011). Of critical importance would be investigations
529 starting from authentic primary or secondary oxidation products suggested in this study as
530 putative intermediates to validate the proposed mechanisms. A novel pathway involving
531 heterogeneous reactions of hydroperoxides followed by hydrolysis/sulfation reactions is
532 proposed to explain the formation of 8 OSs identified in this study; however, more work is
533 also required to examine how acidified sulfate seed aerosols take up organic peroxides from
534 the gas phase and how particle-phase reactions might degrade organic peroxides into low-
535 volatility products such as the OSs.
536

Acknowledgments

The authors thank the Camille and Henry Dreyfus Postdoctoral Fellowship Program in Environmental Chemistry for their financial support. The authors wish also to thank CAPES Foundation, Ministry of Education of Brazil (award no. 99999.000542/2015-06) for their financial support. This study was supported in part by the National Oceanic and Atmospheric Administration (NOAA) Climate Program Office's AC4 program, award no. NA13OAR4310064. The authors wish to thank Kasper Kristensen and Marianne Glasius (Department of Chemistry, Aarhus University, Denmark) who synthesized the 3-pinanol-2-hydrogen sulfate. The authors also thank Tauseef Quraishi, Abid Mahmood, and James Shauer for providing filters collected in Lahore, in addition to the Government of Pakistan, the Pakistani Higher Education Commission, and the United States Agency for International Development (US-AID) for funding field sample collection in Pakistan.

549
550 ## References

551 Atkinson, R.: Atmospheric chemistry of VOCs and NOx, Atmos. Environ., 34, 2063-2101, 2000.
552
553 Atkinson, R., and Arey, J.: Atmospheric degradation of volatile organic compounds, Chem. Rev., 103,
554 4605-4638, 2003.
555
556 Altieri, K.E., Turpin, B.J., and Seitzinger, S.P.: Oligomers, organosulfates, and nitrooxy
557 organosulfates in rainwater identified by ultra-high resolution electrospray ionization FT-ICR mass
558 spectrometry, Atmos. Chem. Phys., 9, 2533-2542, 2009.
559
560 Attygalle, A.B., Garcia-Rubio, S., Ta, J., and Meinwald, J.: Collisionally-induced dissociation mass
561 spectra of organic sulfate anions, J. Chem. Soc., Perkin Trans. 2, 4, 498-506, 2001.
562
563 Boone, E.J., Laskin, A., Laskin, J., Wirth, C., Shepson, P.B., Stirm, B.H., and Pratt, K.A.: Aqueous
564 processing of atmospheric organic particles in cloud water collected via aircraft sampling, Environ.
565 Sci. Technol., 49, 8523-8530, 2015.
566
567 Carrasquillo, A.J., Hunter, J.F., Daumit, K.E., and Kroll, J.H.: Secondary organic aerosol formation
568 via the isolation of individual reactive intermediates: role of alkoxy radical structure, J. Phys. Chem.
569 A, 118, 8807-8816, 2014.
570
571 Cech, N.B., and Enke, C.G.: Practical implications of some recent studies in electrospray ionization
572 fundamentals, Mass Spect. Rev., 20, 362-387, 2001.
573
574 Chacon-Madrid, H.J., Henry, K.M., and Donahue, N.M.: Photo-oxidation of pinonaldehyde at low
575 NOx: from chemistry to organic aerosol formation, Atmos. Chem. Phys., 13, 3227-3236, 2013.
576
577 Chan, M.N., Surratt, J.D., Chan, A.W.H., Schilling, K., Offenberg, J.H., Lewandowski, M., Edney,
578 E.O., Kleindienst, T.E., Jaoui, M., Edgerton, E.S., Tanner, R.L., Shaw, S.L., Zheng, M., Knipping,
579 E.M., and Seinfeld, J.H.: Influence of aerosol acidity on the chemical composition of secondary
580 organic aerosol from β-caryophyllene, Atmos. Chem. Phys., 11, 1735-1751, 2011.
581
582 Claeys, M., Wang, W., Ion, A.C., Kourtchev, I., Gelencsér, A., and Maenhaut, W.: Formation of
583 secondary organic aerosols from isoprene and its gas-phase oxidation products through reaction with
584 hydrogen peroxide, Atmos. Environ., 38, 4093-4098, 2004.

Crounse, J.D., Paulot, F., Kjaergaard, H.G., and Wennberg, P.O.: Peroxy radical isomerization in the oxidation of isoprene, Phys. Chem. Chem. Phys., 13, 13607–13613, 2011.

Crounse, J.D., Nielsen, L.B., Jorgensen, S., Kjaergaard, H.G., and Wennberg, P.O.: Autoxidation of organic compounds in the atmosphere, J. Phys. Chem. Lett, 4, 3513-3520, 2013.

Darer, A.I., Cole-Filipiak, N.C., O'Connor, A.E., and Elrod, M.J.: Formation and stability of atmospherically relevant isoprene-derived organosulfates and organonitrates, Environ. Sci. Technol., 45, 1895–1902, 2011.

Docherty, K.S., Wu, W., Lim, Y.B., and Ziemann, P.J.: Contributions of organic peroxides to secondary aerosol formed from reactions of monoterpenes with O_3, Environ. Sci. Technol., 39, 4049-4059, 2005.

Ehn, M., Thornton, J.A., Kleist, E., Sipilä, M., Junninen, H., Pullinen, I., Springer, M., Rubach, F., Tillmann, R., Lee, B., Lopez- Hilfiker, F., Andres, S., Acir, I.-H., Rissanen, M., Jokinen, T., Schobesberger, S., Kangasluoma, J., Kontkanen, J., Nieminen, T., Kurten, T., Nielsen, L.B., Jorgensen, S., Kjaergaard, H.G., Canagaratna, M., Maso, M.D., Berndt, T., Petaja, T., Wahner, A., Kerminen, V.-M., Kulmala, M., Worsnop, D.R., Wildt, J., and Mentel, T.F.: A large source of low-volatility secondary organic aerosol, Nature, 506, 476–479, 2014.

Elder, A., and Oberdörster, G.: Translocation and effects of ultrafine particles outside of the lung, Clin. Occup. Environ. Med., 5, 785-796, 2006.

Fraser, M.P., Cass, G.R., Simoneit, B.R.T, and Rasmussen, R.A.: Air quality model evaluation data for organics. 4. C2-C36 non- aromatic hydrocarbons, Environ. Sci. Technol., 31, 2356-2367, 1997.

Gaston, C.J., Riedel, T.P., Zhang, Z., Gold, A., Surratt, J.D., and Thornton, J.A: Reactive uptake of an isoprene-derived epoxydiol to submicron aerosol particles, Environ. Sci. Technol., 48, 11178-11186, 2014.

Gentner, D.R., Isaacman, G., Worton, D.R., Chan, A.W.H., Dallmann, T.R., Davis, L., Liu, S., Day, D.A., Russell, L.M., Wilson, K.R., Weber, R., Guha, A., Harley, R.A., and Goldstein, A.H.: Elucidating secondary organic aerosol from diesel and gasoline vehicles through detailed characterization of organic carbon emissions. Proc. Natl. Acad. Sci., 109, 18318–18323, 2012.

622 Gómez-González, Y., Surratt, J.D., Cuyckens, F., Szmigielski, R., Vermeylen, R., Jaoui, M.,
623 Lewandowski, M., Offenberg, J.H., Kleindienst, T.E., Edney, E.O., Blockhuys, F., Van Alsenoy, C.,
624 Maenhaut, W., and Claeys, M.: Characterization of organosulfates from the photooxidation of
625 isoprene and unsaturated fatty acids in ambient aerosol using liquid chromatography/(-) electrospray
626 ionization mass spectrometry, J. Mass Spect., 43, 371-382, 2008.
627
628 Hallquist, M., Wenger, J.C., Baltensperger, U., Rudich, Y., Simpson, D., Claeys, M., Dommen, J.,
629 Donahue, N.M., George, C., Goldstein, A.H., Hamilton, J.F., Herrmann, H., Hoffmann, T., Iinuma, Y.,
630 Jang, M., Jenkin, M.E., Jimenez, J.L., Kiendler-Scharr, A., Maenhaut, W., McFiggans, G., Mentel,
631 T.F., Monod, A., Prévôt, A.S.H., Seinfeld, J.H., Surratt, J.D., Szmigielski, R., and Wildt, J.: The
632 formation, properties and impact of secondary organic aerosol: current and emerging issues, Atmos.
633 Chem. Phys., 9, 5155-5236, 2009.
634
635 Hansen, A.M.K., Kristensen, K., Nguyen, Q.T., Zare, A., Cozzi, F., Nøjgaard, J.K., Skov, H., Brandt,
636 J., Christensen, J.H., Ström, J., Tunved, P., Krejci, R., and Glasius, M.: Organosulfates and organic
637 acids in Arctic aerosols: Speciation, annual variation and concentration levels, Atmos. Chem. Phys.,
638 14, 7807-7823, 2014.
639
640 Hatch, L.E., Creamean, J.M., Ault, A.P., Surratt, J.D., Chan, M.N., Seinfeld, J.H., Edgerton, E.S., Su,
641 Y., and Prather, K.A.: Measurements of isoprene-derived organosulfates in ambient aerosols by
642 aerosol time-of-flight mass spectrometry - Part 1: Single particle atmospheric observations in Atlanta,
643 Environ. Sci. Technol., 45, 5105-5111.
644
645 Hayes, P.L., Ortega, A.M., Cubison, M.J., Froyd, K.D., Zhao, Y., Cliff, S.S., Hu, W.W., Toohey,
646 D.W., Flynn, J.H., Lefer, B.L., Grossberg, N., Alvarez, S., Rappenglück, B., Taylor, J.W., Allan, J.D.,
647 Holloway, J.S., Gilman, J.B., Kuster, W.C., De Gouw, J.A., Massoli, P., Zhang, X., Liu, J., Weber,
648 R.J., Corrigan, A.L., Russell, L.M., Isaacman, G., Worton, D.R., Kreisberg, N.M., Goldstein, A.H.,
649 Thalman, R., Waxman, E.M., Volkamer, R., Lin, Y.H., Surratt, J.D., Kleindienst, T.E., Offenberg,
650 J.H., Dusanter, S., Griffith, S., Stevens, P.S., Brioude, J., Angevine, W.M., and Jimenez, J.L.: Organic
651 aerosol composition and sources in Pasadena, California, during the 2010 CalNex campaign, J.
652 Geophys. Res. Atmos., 118, 9233-9257, 2013.
653
654 Hawkins, L.N., Russell, L.M., Covert, D. S., Quinn, P. K., and Bates, T. S.: Carboxylic acids, sulfates,
655 and organosulfates in processed continental organic aerosol over the south east Pacific Ocean during
656 VOCALS-REx 2008, J. Geophys. Res.-Atmos., 115, D13201, 2010.
657

Hu, K.S., Darer, A.I., and Elrod, M.J.: Thermodynamics and kinetics of the hydrolysis of atmospherically relevant organonitrates and organosulfates, Atmos. Chem. Phys., 11, 8307–8320, 2011.

Hunter, J.F., Carrasquillo, A.J., Daumit, K.E., and Kroll, J.H.: Secondary organic aerosol formation from acyclic, monocyclic, and polycyclic alkanes, Environ. Sci. Technol., 48, 10227-10234, 2014.

Iinuma, Y., Müller, C., Berndt, T., Böge, O., Claeys, M., and Herrmann, H.: Evidence for the existence of organosulfates from β-pinene ozonolysis in ambient secondary organic aerosol, Environ. Sci. Tech., 41, 6678-6683, 2007.

Iinuma, Y., Böge, O., Kahnt, A., and Herrmann, H.: Laboratory chamber studies on the formation of organosulfates from reactive uptake of monoterpene oxides, Phys. Chem. Chem. Phys., 11, 7985-7997, 2009.

Jacobs, M.I., Darer, A.I., and Elrod, M.J.: Rate constants and products of the OH reaction with isoprene-derived epoxides, Environ. Sci. Technol, 43, 12868-12876, 2013.

Jokinen, T., Sipilä, M., Richters, S., Kerminen, V.-M., Paasonen, P., Stratmann, F., Worsnop, D., Kulmala, M., Ehn, M., Herrmann, H., and Berndt, T.: Rapid Autoxidation Forms Highly Oxidized RO2 Radicals in the Atmosphere, Angwe. Chem. Internat. Ed., 53, 14596–14600, 2014.

Kamens, R.M., Zhang, H., Chen, E.H., Zhou, Y., Parikh, H.M., Wilson, R.L., Galloway, K.E., and Rosen, E.P.: Secondary organic aerosol formation from toluene in an atmospheric hydrocarbon mixture: water and particle seed effects, Atmos. Environ., 45, 2324-2334, 2011.

Kitanovski, Z., Grgic, I., Yasmeen, F., Claeys, M., and Cusak, A.: Development of a liquid chromatographic method based on ultraviolet–visible and electrospray ionization mass spectrometric detection for the identification of nitrocatechols and related tracers in biomass burning atmospheric organic aerosol, Rapid Commun. Mass. Spectrom., 26, 793-804, 2012.

Kristensen, K., and Glasius, M.: Organosulfates and oxidation products from biogenic hydrocarbons in fine aerosols from a forest in North West Europe during spring, Atmos. Environ., 45, 4546-4556, 2011.

693 Kroll, J.H., and Seinfeld, J.H.: Chemistry of secondary organic aerosol: formation and evolution of
694 low-volatility organics in the atmosphere, Atmos. Environ., 42, 3593-3624, 2008.
695
696 Kuang, B.Y., Lin, P., Hub, M., and Yu, J.Z.: Aerosol size distribution characteristics of organosulfates
697 in the Pearl River Delta region, China, Atmos. Environ., 130, 23-35, 2016.
698
699 Kundu, S., Quraishi, T.A., Yu, G., Suarez, C., Keutsch, F.N., and Stone, E.A.: Evidence and
700 quantification of aromatic organosulfates in ambient aerosols in Lahore, Pakistan, Atmos. Chem.
701 Phys., 13, 4865-4875, 2013.
702
703 Kwok, E.S.C., and Atkinson, R.: Estimation of hydroxyl radical reaction rate constants for gas-phase
704 organic compounds using a structure-reactivity relationship: an update, Atmos. Environ., 29, 1685-
705 1695, 1995.
706
707 Lambe, A.T., Onasch, T.B., Croasdale, D.R., Wright, J.P., Martin, A.T., Franklin, J.P., Massoli, P.,
708 Kroll, J.H., Canagaratna, M.R., Brune, W.H., Worsnop, D.R., and Davidovits, P.: Transitions from
709 functionalization to fragmentation reactions of laboratory secondary organic aerosol (SOA) Generated
710 from the OH oxidation of alkane precursors, Environ. Sci. Technol., 46, 5430-5437, 2012.
711
712 Lee, S., Jang, M., and Kamens, R. K.: SOA formation from the photooxidation of α-pinene in the
713 presence of freshly emitted diesel soot exhaust, Atmos. Environ., 38, 2597–2605, 2004.
714
715 Liao, J., Froyd, K.D., Murphy, D.M., Keutsch, F.N., Yu, G., Wennberg, P.O., St. Clair, J.M., Crounse,
716 J.D., Wisthaler, A., Mikoviny, T., Jimenez, J.L., Campuzano-Jost, P., Day, D.A., Hu, W., Ryerson,
717 T.B., Pollack, I.B., Peischl, J., Anderson, B.E., Ziemba, L.D., Blake, D.R., Meinardi, S., and Diskin,
718 G.: Airborne measurements of organosulfates over the continental U.S., J. Geophys. Res. D, 120,
719 2990-3005, 2015.
720
721 Liggio, J., and Li, S.-M.: Organosulfate formation during the uptake of pinonaldehyde on acidic
722 sulfate aerosols, Geophys. Res. Lett., 33, L13808, 2006.
723
724 Lim, Y.B., and Ziemann, P.J.: Products and mechanism of secondary organic aerosol formation from
725 reactions of n-alkanes with OH radicals in the presence of NOx, Environ. Sci. Technol., 39, 9229-
726 9236, 2005.
727

728 Lim, Y.B., and Ziemann, P.J.: Effects of molecular structure on aerosol yields from OH radical-
729 initiated reactions of linear, branched, and cyclic alkanes in the presence of NOx, Environ. Sci.
730 Technol., 43, 2328-2334, 2009.
731
732 Lin, Y.-H., Zhang, Z., Docherty, K.S., Zhang, H., Budisulistiorini, S.H., Rubitschun, C.L., Shaw, S.L.,
733 Knipping, E.M., Edgerton, E.S., Kleindienst, T.E., Gold, A., and Surratt, J.D.: Isoprene epoxydiols as
734 precursors to secondary organic aerosol formation: acid-catalyzed reactive uptake studies with
735 authentic compounds, Environ. Sci. Technol., 46, 250-258, 2012.
736
737 Lin, Y.-H., Budisulistiorini, S.H., Chu, K., Siejack, R.A., Zhang, H., Riva, M., Zhang, Z., Gold, A.,
738 Kautzman, K.E., and Surratt, J.D.: Light-absorbing oligomer formation in secondary organic aerosol
739 from reactive uptake of isoprene epoxydiols, Environ. Sci. Technol., 48, 12012-12021, 2014.
740
741 Loza, C.L., Craven, J.S., Yee, L.D., Coggon, M.M., Schwantes, R.H., Shiraiwa, M., Zhang, X.,
742 Schilling, K.A., Ng, N.L., Canagaratna, M.R., Ziemann, P., Flagan, R.C., and Seinfeld, J.H.:
743 Secondary organic aerosol yields of 12-carbon alkanes, Atmos. Chem. Phys., 7, 1423-1439, 2014.
744
745 Ma, Y., Xu, X., Song, W., Geng, F., and Wang, L.: Seasonal and diurnal variations of particulate
746 organosulfates in urban Shanghai, China, Atmos. Environ., 85, 152-160, 2014.
747
748 Mael, L.E., Jacobs, M.I., and Elrod, M.J.: Organosulfate and nitrate formation and reactivity from
749 epoxides derived from 2-methyl-3-buten-2-ol, J. Phys. Chem. A, 119, 4464-4472, 2015.
750
751 Mentel, T.F., Springer, M., Ehn, M., Kleist, E., Pullinen, I., Kurten, T., Rissanen, M., Wahner, A., and
752 Wildt, J.: Formation of highly oxidized multifunctional compounds: autoxidation of peroxy radicals
753 formed in the ozonolysis of alkenes –deduced from structure–product relationships, Atmos. Chem.
754 Phys., 15, 6745-6765, 2015.
755
756 Mutzel, A., Poulain, L., Berndt, T., Iinuma, Y., Rodigast, M., Böge, O., Richters, S., Spindler, G.,
757 Sipila, M., Jokinen, T., Kulmala, M., and Herrmann, H.: Highly oxidized multifunctional organic
758 compounds observed in tropospheric particles: a field and laboratory study, Environ. Sci. Technol., 49,
759 7754-7761, 2015.
760
761 Ng, N.L., Kwan, A.J., Surratt, J.D., Chan, A.W.H., Chhabra, P.S., Sorooshian, A., Pye, H.O.T.,
762 Crounse, J.D., Wennberg, P.O., Flagan, R.C., and Seinfeld, J.H.: Secondary organic aerosol (SOA)
763 formation from reaction of isoprene with nitrate radicals (NO_3), Atmos. Chem. Phys., 8, 4117-4140,
764 2008.

765 Nozière, B., Ekström, S., Alsberg, T., and Holmström, S.: Radical-initiated formation of
766 organosulfates and surfactants in atmospheric aerosols, Geophys. Res. Lett., 37, L05806, 2010.
767
768 Orlando, J.J., and Tyndall, G.S.: Laboratory studies of organic peroxy radical chemistry: an overview
769 with emphasis on recent issues of atmospheric significance, Chem Rev., 41, 6294-6317, 2012.
770
771 Paulot, F., Crounse, J.D., Kjaergaard, H.G., Kroll, J.H., Seinfeld, J.H., and Wennberg, P.O.: Isoprene
772 photooxidation: New insights into the production of acids and organic nitrates, Atmos. Chem. Phys.,
773 9, 1479-1501, 2009.
774
775 Pratt, K.A., Fiddler, M.N., Shepson, P.B., Carlton, A.G, and Surratt, J.D.: Organosulfates in cloud
776 water above the Ozarks isoprene source region, Atmos. Environ., 77, 231-238, 2013.
777
778 Presto, A.A., Miracolo, M.A., Donahue, N.M., and Robinson, A.L.: Secondary organic aerosol
779 formation from high-NOx Photo-oxidation of low volatility precursors: N-alkanes, Environ. Sci.
780 Technol.,44, 2029-2034, 2010
781
782 Pye, H.O.T., and Pouliot, G.A.: Modeling the role of alkanes, polycyclic aromatic hydrocarbons, and
783 their oligomers in secondary organic aerosol formation, Environ. Sci. Technol., 46, 6041-6047, 2012.
784 Raff, J.D., and Finlayson-Pitts, B.J.: Hydroxyl radical quantum yields from isopropyl nitrite photolysis
785 in air, Environ. Sci. Technol., 44, 8150-8155, 2010.
786
787 Riedel, T.P., Lin, Y., Budisulistiorini, S.H., Gaston, C.J., Thornton, J.A., Zhang, Z., Vizuete, W.,
788 Gold, D., and Surratt, J.D.: Heterogeneous reactions of isoprene-derived epoxides: reaction
789 probabilities and molar secondary organic aerosol yield estimates, Environ. Sci. Technol. Lett., 2, 38-
790 42, 2015.
791
792 Rissanen, M.P., Kurten, T., Sipila, M., Thornton, J.A., Kausiala, O., Garmash, O., Kjaergaard, H.G.,
793 Petaja, T., Worsnop, D.R., Ehn, M., and Kulmala, M.: Effects of chemical complexity on the
794 autoxidation mechanisms of endocyclic alkene ozonolysis products: from methylcyclohexenes toward
795 understanding α-pinene, J. Phys. Chem. A, 119, 4633-4650, 2015.
796
797 Riva, M., Tomaz, S., Cui, T., Lin, Y.-H., Perraudin, E., Gold, A., Stone, E.A., Villenave, E., and
798 Surratt, J.D.: Evidence for an unrecognized secondary anthropogenic source of organosulfates and
799 sulfonates: Gas-phase oxidation of polycyclic aromatic hydrocarbons in the presence of sulfate
800 aerosol, Environ. Sci. Technol., 49, 6654–6664, 2015a.

Riva, M., Budisulistiorini, S.H., Zhang, Z., Gold, A., and Surratt, J.D.: Chemical characterization of secondary organic aerosol constituents from isoprene ozonolysis in the presence of acidic aerosol, Atmos. Chem., 130, 5-13, 2016.

Robinson, A.L., Donahue, N.M., Shrivastava, M.K., Weitkamp, E., Sage, A.M., Grieshop, A. P., Lane, T.E., Pierce, J.R., and Pandis, S.N.: Rethinking organic aerosols: semivolatile emissions and photochemical aging, Science, 315, 1259–1262, 2007.

Romero, F., and Oehme, M.: Organosulfates – a new component of humic-like substances in atmospheric aerosols?, J. Atmos. Chem., 52, 283-294, 2005.

Rudzinski, K. J., Gmachowski, L., and Kuznietsova, I.: Reactions of isoprene and sulphoxy radical-anions – a possible source of atmospheric organosulphites and organosulphates, Atmos. Chem. Phys., 9, 2129-2140, 2009.

Schilling Fahnestock, K.A., Yee, L.D., Loza, C.L., Coggon, M.M., Schwantes, R., Zhang, X., Dalleska, N.F., and Seinfeld, J.H.: Secondary organic aerosol composition from C12 alkanes, J. Phys. Chem. A, 119, 4281-4297, 2015.

Schindelka, J., Iinuma, Y., Hoffmann, D., and Herrmann, H.: Sulfate radical-initiated formation of isoprene-derived organosulfates in atmospheric aerosols, Faraday Discuss., 165, 237-259, 2013.

Schöne, L., Schindelka, J., Szeremeta, E., Schaefer, T., Hoffmann, D., Rudzinski, K.J., Szmigielski, R., and Herrmann, H.: Atmospheric aqueous phase radical chemistry of the isoprene oxidation products methacrolein, methyl vinyl ketone, methacrylic acid and acrylic acid – kinetics and product studies, Phys. Chem. Chem. Phys., 16, 6257–6272, 2014

Shalamzari, S.M., Ryabtsova, O., Kahnt, A., Vermeylen, R., Hérent, M.-F., Quetin-Leclercq, J., Van Der Veken, P., Maenhaut, W., and Claeys, M.: Mass spectrometric characterization of organosulfates related to secondary organic aerosol from isoprene, Rapid Commun. Mass Spectrom., 27, 784-794, 2013.

Shalamzari, M.S., Kahnt, A., Vermeylen, R., Kleindienst, T.E., Lewandowski, M., Cuyckens, F., Maenhaut,W., and Claeys, M.: Characterization of polar organosulfates in secondary organic aerosol from the green leaf volatile 3-Z-hexenal, Environ. Sci. Technol., 48, 12671–12678, 2014.

837 Shalamzari, M.S., Vermeylen, R., Blockhuys, F., Kleindienst, T.E., Lewandowski, M., Szmigielski,
838 R., Rudzinski, K.J., Spolnik, G., Danikiewicz, W., Maenhaut,W., and Claeys, M.: Characterization of
839 polar organosulfates in secondary organic aerosol from the unsaturated aldehydes 2-E-pentenal, 2-E-
840 hexenal, and 3-Z-hexenal, Atmos. Chem. Phys. Discuss., 15, 29555–29590, 2015.
841
842 Stevens, B., and Boucher, O.: The aerosol effect, Nature, 490, 40-41, 2012.
843
844 Stone, E., Schauer, J., Quraishi, T.A., and Mahmood, A.: Chemical characterization and source
845 apportionment of fine and coarse particulate matter in Lahore, Pakistan, Atmos. Environ., 44, 1062-
846 1070, 2010.
847
848 Stone, E.A., Yang, L., Yu, L.E., and Rupakheti, M.: Characterization of organosulfate in atmospheric
849 aerosols at Four Asian locations, Atmos. Environ., 47, 323-329, 2012.
850
851 Surratt, J.D., Murphy, S.M., Kroll, J.H., Ng, N.L., Hildebrandt, L., Sorooshian, A., Szmigielski, R.,
852 Vermeylen, R., Maenhaut, W., Claeys, M., Flagan, R.C., and Seinfeld, J.H.: Chemical composition
853 of secondary organic aerosol formed from the photooxidation of isoprene, J. Phys. Chem. A, 110,
854 9665-9690, 2006.
855
856 Surratt, J.D., Kroll, J.H., Kleindienst, T.E., Edney, E.O., Claeys, M., Sorooshian, A., Ng, N.L.,
857 Offenberg, J.H., Lewandowski, M., Jaoui, M., Flagan, R.C., and Seinfeld, J.H.: Evidence for
858 organosulfates in secondary organic aerosol, Environ. Sci. Technol., 41, 517-527, 2007.
859
860 Surratt, J.D., Gómez-González, Y., Chan, A.W.H., Vermeylen, R., Shahgholi, M., Kleindienst, T.E.,
861 Edney, E.O., Offenberg, J.H., Lewandowski, M., Jaoui, M., Maenhaut, W., Claeys, M., Flagan, R.C.,
862 and Seinfeld, J.H.: Organosulfate formation in biogenic secondary organic aerosol, J. Phys. Chem. A,
863 112, 8345-8378, 2008.
864
865 Surratt, J.D., Chan, A.W.H., Eddingsaas, N.C., Chan, M., Loza, C.L., Kwan, A.J., Hersey, S.P.,
866 Flagan, R.C., Wennberg, P.O., and Seinfeld, J.H.: Reactive intermediates revealed in secondary
867 organic aerosol formation from isoprene, Proc. Natl. Acad. Sci., 107, 6640-6645, 2010.
868
869 Tao, S., Lu, X., Levac, N., Bateman, A.P., Nguyen, T.B., Bones, D.L., Nizkorodov, S.A., Laskin, J.,
870 Laskin, A., and Yang, X.: Molecular characterization of organosulfates in organic aerosols from
871 Shanghai and Los Angeles urban areas by nanospray-desorption electrospray ionization high-
872 resolution mass spectrometry, Environ. Sci. Technol., 48 (18), 10993-11001, 2014.
873

874 Tkacik, D.S., Presto, A.A., Donahue, N.M., and Robinson, A.L.: Secondary organic aerosol formation
875 from intermediate-volatility organic compounds: cyclic, linear, and branched alkanes, Environ. Sci.
876 Technol., 46, 8773-8781, 2012.
877
878 Tolocka, M.P., and Turpin, B.: Contribution of organosulfur compounds to organic aerosol mass,
879 Environ. Sci. Technol., 46, 7978-7983, 2012.
880
881 Wang, L., Arey, J., and Atkinson, R.: Kinetics and products of photolysis and reaction with OH
882 radicals of a series of aromatic carbonyl compounds, Environ. Sci. Technol., 40, 5465-5471, 2006.
883
884 Wang, X.K., Rossignol, S., Ma, Y, Yao, L., Wang, M.Y., Chen, J.M., George, C., and Wang, L.:
885 Identification of particulate organosulfates in three megacities at the middle and lower reaches of the
886 Yangtze River, Atmos. Chem. Phys. Discuss., 15, 21414-21448, 2015.
887
888 Witkowski, B., and Gierczak, T.: Analysis of α-acyloxyhydroperoxy aldehydes with electrospray
889 ionization–tandem mass spectrometry (ESI-MSn), J. Mass. Spectrom., 48, 79-88, 2013.
890
891 Yao, L., Ma, Y., Wang, L., Zheng, J., Khalizov, A., Chen, M., Zhou, Y., Qi, L., and Cui, F.: Role of
892 stabilized Criegee Intermediate in secondary organic aerosol formation from the ozonolysis of α-
893 cedrene, Atmos. Environ., 94, 448-457, 2014.
894
895 Yee, L.D., Craven, J.S., Loza, C.L., Schilling, K.A., Ng, N.L., Canagaratna, M.R., Ziemann, P.J.,
896 Flagan, R.C., and Seinfeld, J.H.: Secondary organic aerosol formation from low-NO x photooxidation
897 of dodecane: Evolution of multigeneration gas-phase chemistry and aerosol composition, J. Phys.
898 Chem. A, 116, 6211-6230, 2012.
899
900 Yee, L.D., Craven, J.S., Loza, C.L., Schilling, K.A., Ng, N.L., Canagaratna, M.R., Ziemann, P.J.,
901 Flagan, R.C., and Seinfeld, J.H.: Effect of chemical structure on secondary organic aerosol formation
902 from C12 alkanes, Atmos. Chem. Phys., 13, 11121-11140, 2013.
903
904 Zhang, H., Worton, D.R., Lewandowski, M., Ortega, J., Rubitschun, C.L., Park, J.-H., Kristensen, K.,
905 Campuzano-Jost, P., Day, D.A., Jimenez, J.L., Jaoui, M., Offenberg, J.H., Kleindienst, T.E., Gilman,
906 J., Kuster, W.C., De Gouw, J., Park, C., Schade, G.W., Frossard, A.A., Russell, L., Kaser, L., Jud, W.,
907 Hansel, A., Cappellin, L., Karl, T., Glasius, M., Guenther, A., Goldstein, A.H., Seinfeld, J.H., Gold,
908 A., Kamens, R.M., and Surratt, J.D.: Organosulfates as tracers for secondary organic aerosol (SOA)

formation from 2-methyl-3-buten-2-ol (MBO) in the atmosphere, Environ. Sci. Technol., 46, 9437-9446, 2012.

Zhang, X., Schwantes, R.H., Coggon, M.M., Loza, C.L., Schilling, K.A., Flagan, R.C., Seinfeld, J.H.: Role of ozone in SOA formation from alkane photooxidation, Atmos. Phys. Chem., 14, 1733-1753, 2014

Zhang, X., McVay, R.C., Huang, D.D., Dalleska, N.F., Aumont, B., Flagan, R.C., and Seinfeld, J.H.: Formation and evolution of molecular products in α-pinene secondary organic aerosol, Proc. Natl. Acad. Sci., 112, 14168-14173, 2015.

Ziemann, P.J., and Atkinson, R.: Kinetics, products, and mechanisms of secondary organic aerosol formation, Chem. Soc. Rev., 41, 6582-6605, 2012.

922 **Table 1.** Summary of outdoor smog chamber conditions used for the photooxidation of long-chain alkanes using isopropyl nitrite (IPN) as an OH
923 radical precursor.
924

Hydrocarbons (HCs)	Initial [HC] (ppb)	Chamber Side	Seed aerosol	Initial [IPN] (ppb)	[NO] (ppb)	[O_3] (ppb)	T (K)	RH (%)	Final OA mass (μg m^{-3})	Total Peroxides (μg m^{-3})
Dodecane	412	N	Non-Acidified	215	< 1	512	304-311	49-59	58	*N.d.*
	420	S	Acidified	212	< 1	528	305-311	51-63	65	*N.d.*
Dodecane	422	N	Non-Acidified	215	< 1	507	302-308	15-20	49	*N.d.*
	427	S	Acidified	212	< 1	538	303-308	14-17	53	*N.d.*
Dodecane	397	N	Acidified	215	< 1	506	304-309	45-52	52	15.4
	409	S	Acidified	212	< 1	585	305-310	15-19	59	15.2
Decalin	175	N	Non-Acidified	138	< 1	327	302-309	48-45	204	*N.d.*
	180	S	Acidified	136	< 1	335	302-308	51-49	224	*N.d.*
Decalin	199	N	Non-Acidified	138	< 1	317	305-306	13-13	200	59.7
	204	S	Acidified	136	< 1	328	306-306	13-14	211	75.5
Decalin	N.I.	N	Acidified	138	< 1	319	302-306	43-54	245	43.9
	N.I.	S	Acidified	136	< 1	324	301-306	9-12	270	57.8
Cyclodecane	257	N	Non-Acidified	172	< 1	374	298-301	53-61	218	76.6
	263	S	Acidified	170	< 1	364	299-301	52-60	238	72.2
Cyclodecane	256	N	Non-Acidified	172	< 1	350	300-303	13-15	177	57.8
	261	S	Acidified	170	< 1	332	300-302	13-14	210	68.3
Cyclodecane	245	N	Acidified	172	< 1	345	298-300	10-11	259	78.8
	250	S	Acidified	170	< 1	355	299-300	51-49	270	69.2

925 *N and S design "North chamber" and "South Chamber", respectively; N.I.: No Information, N.d. Not determined*
926

Table 2. Concentrations (ng m^{-3}) of OSs identified in laboratory-generated dodecane, decalin and cyclodecane SOA and in fine aerosol collected from two urban locations.

		Lahore, Pakistan					Pasadena, USA							
$[M - H]^-$	Precursors	04-30-2007	05-06-2007	05-12-2007	11-02-2007	11-08-2007	05-17-2010	05-18-2010	05-19-2010	05-23-2010	05-24-2010	05-25-2010	05-28-2010	06-11-2010
$C_7H_{13}O_5S^-$ (209.0472)[a,b]	Dodecane	7.53	6.53	4.24	6.35	9.66	*N.d.*	*N.d.*	0.27	0.07	0.10	*N.d.*	0.09	0.21
$C_9H_{17}O_5S^-$ (237.0786)[a,b]	Dodecane	9.35	6.81	4.27	7.27	12.40	0.13	0.15	0.30	0.10	0.16	0.16	0.13	0.25
$C_{10}H_{19}O_5S^-$ (251.0946)[a,c]	Cyclodecane	10.40	7.51	4.08	13.17	20.96	*N.d.*	*N.d.*	*N.d.*	*N.d.*	*N.d.*	*N.d.*	*N.d.*	*N.d.*
$C_{10}H_{17}O_6S^-$ (265.079)[a,c]	Cyclodecane	2.83	2.45	2.15	2.86	7.63	0.18	0.21	0.35	0.14	0.15	0.16	0.15	0.36
$C_9H_{15}O_7S^-$ (267.0554)[a,c]	Decalin	0.98	1.87	1.93	2.19	6.53	0.21	0.21	0.58	0.11	0.21	0.20	0.16	0.40
$C_9H_{17}O_7S^-$ (269.0700)[a,b]	Decalin	2.04	3.02	2.22	2.62	7.56	0.42	0.38	0.58	0.26	0.40	0.38	0.35	0.56
$C_{10}H_{15}O_7S^-$ (279.0556)[a,c]	Cyclodecane	6.38	20.25	21.97	15.06	35.93	0.14	0.21	0.54	0.10	0.19	0.21	0.20	0.29
$C_{12}H_{23}O_5S^-$ (279.1272)[c,d]	Dodecane	14.57	12.18	3.41	9.50	19.56	*N.d.*	*N.d.*	*N.d.*	*N.d.*	*N.d.*	*N.d.*	*N.d.*	*N.d.*
$C_9H_{17}O_8S^-$ (285.0651)[a,c]	Decalin	*N.d.*	0.61	*N.d.*	*N.d.*	1.44	0.20	0.09	0.21	0.05	0.08	0.09	0.03	0.17
$C_{10}H_{15}O_8S$- (295.0500)[a,c]	Decalin	*N.d.*	0.53	0.48	0.54	3.78	0.17	0.22	0.65	0.08	0.17	0.24	0.19	0.52
$C_{10}H_{17}O_8S^-$ (297.0650)[a,c]	Decalin	*N.d.*	0.78	0.92	0.69	*N.d.*	0.13	0.08	0.43	0.07	0.10	0.09	0.10	0.24
$C_{10}H_{16}NO_9S^-$ (326.0550)[a,c]	Decalin	0.25	0.32	0.21	*N.d.*	*N.d.*	*N.d.*	0.13	0.22	0.06	0.09	0.11	0.12	0.11

[a] Quantified using authentic OS (3-pinanol-2-hydrogen sulfate, $C_9H_{13}O_6S^-$), [b] OSs belonging to group 2, [c] OSs belonging to group 1, [d] quantified using octyl sulfate OS ($C_8H_{17}O_4S^-$). Different isomers for one ion have been summed; N.d.: not detected.

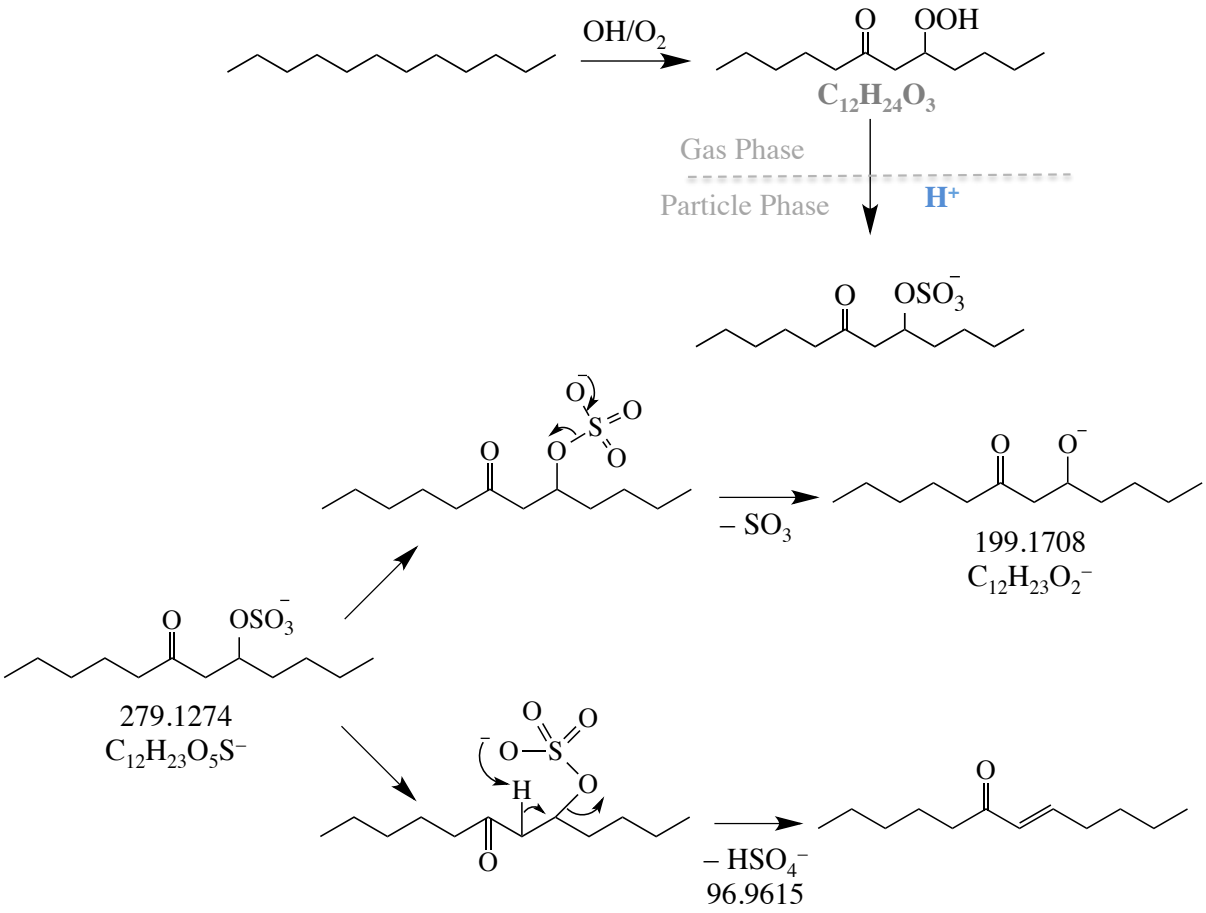

Figure 1. Proposed formation pathway of OS-279 (*m/z* 279.1274) and its corresponding fragmentation routes. The suggested mechanism is based on identified products from previous study (Yee et al., 2012).

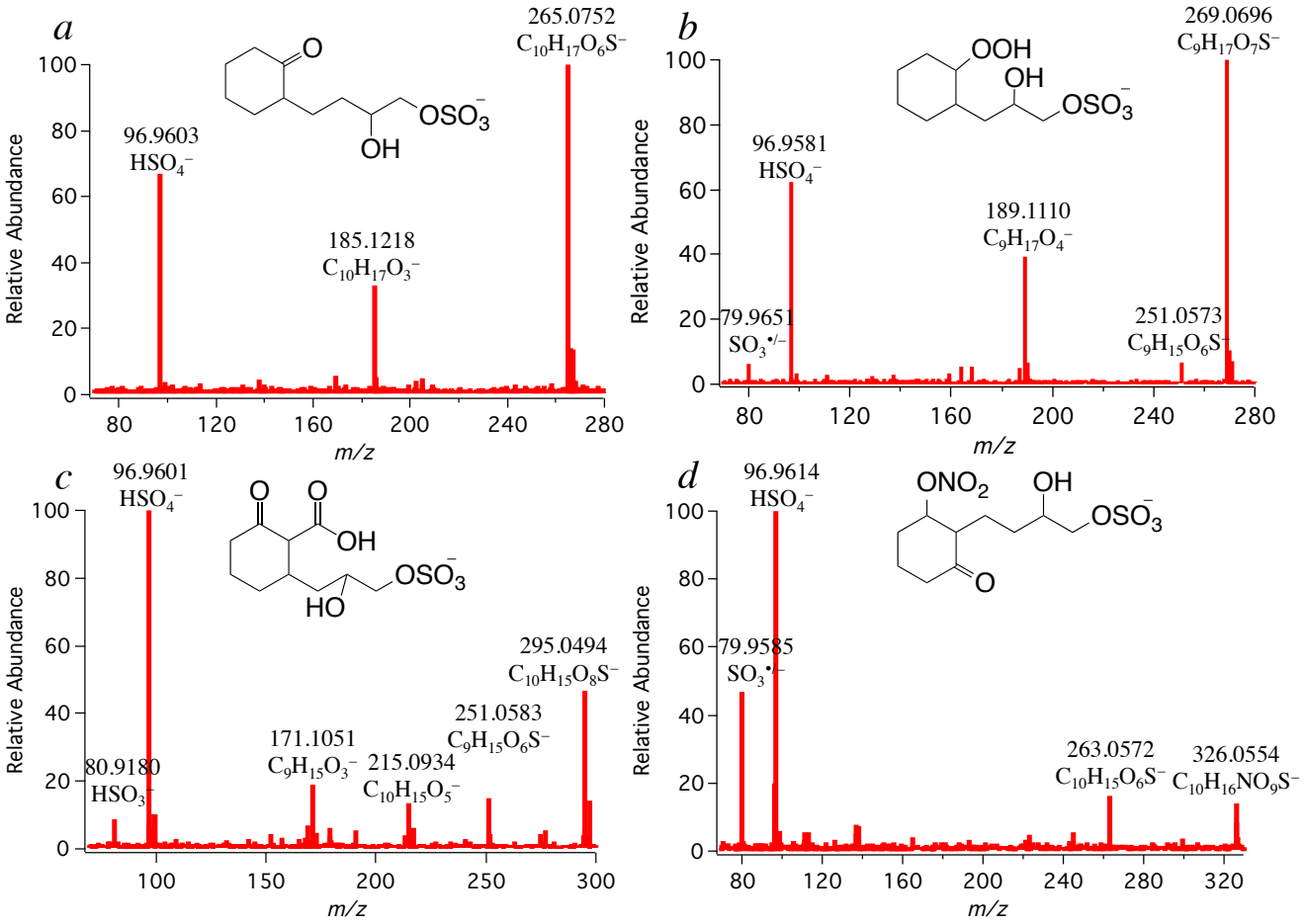

Figure 2. MS^2 spectra obtained for selected decalin-derived OSs: (*a*) *m/z* 265.0752 ($C_{10}H_{17}O_6S^-$), (*b*) *m/z* 269.0696 ($C_9H_{17}O_7S^-$), (*c*) *m/z* 295.0494 ($C_{10}H_{15}O_8S^-$) and (*d*) *m/z* 326.0554 ($C_{10}H_{16}NO_9S^-$). Fragmentation schemes are proposed in Figure S2.

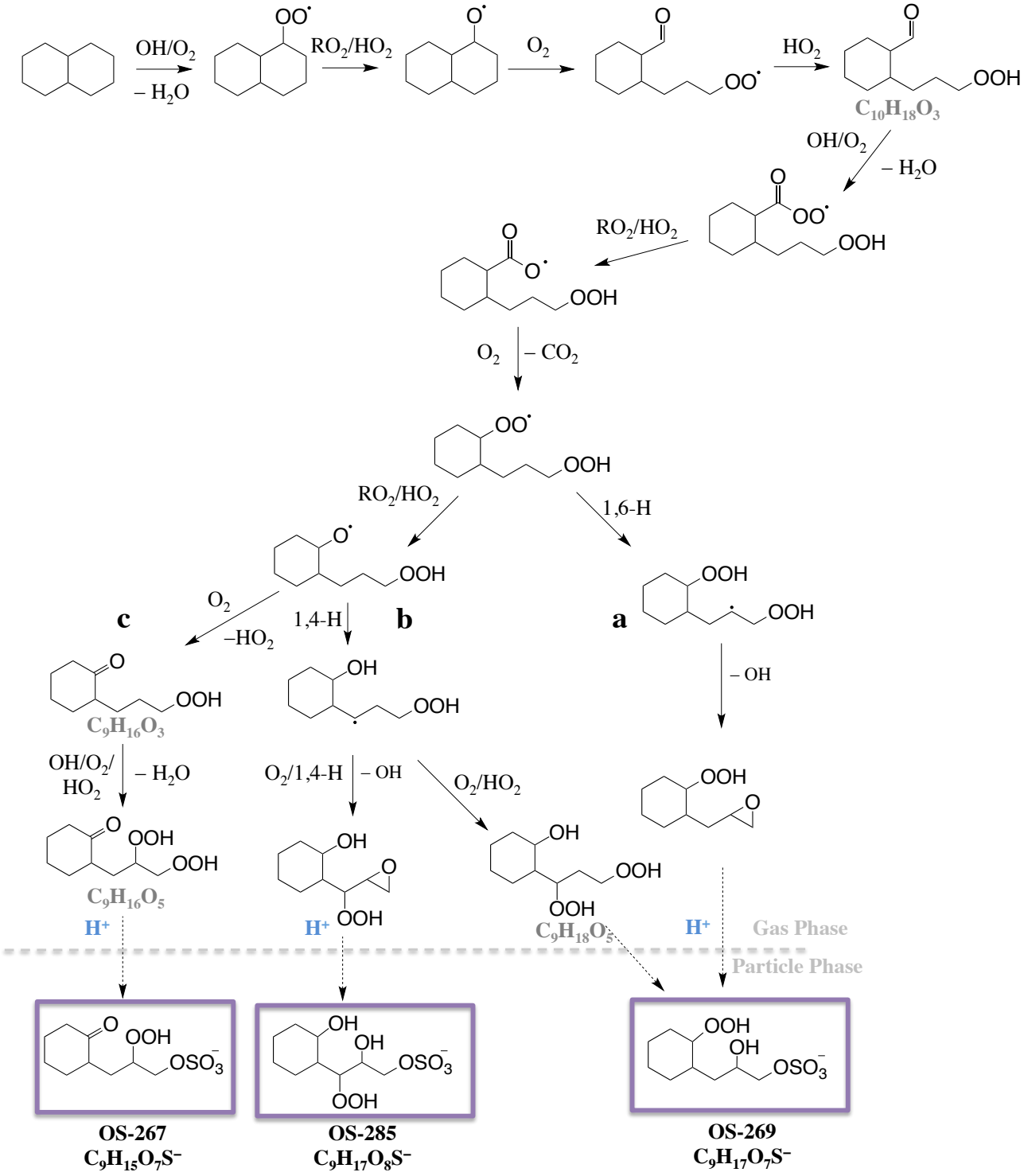

Figure 3. Tentatively proposed formation pathways of OS-267 (*m/z* 267.9552), OS-269 (*m/z* 269.0696) and OS-285 (285.0654) from the oxidation of decalin in presence of sulfate aerosol.

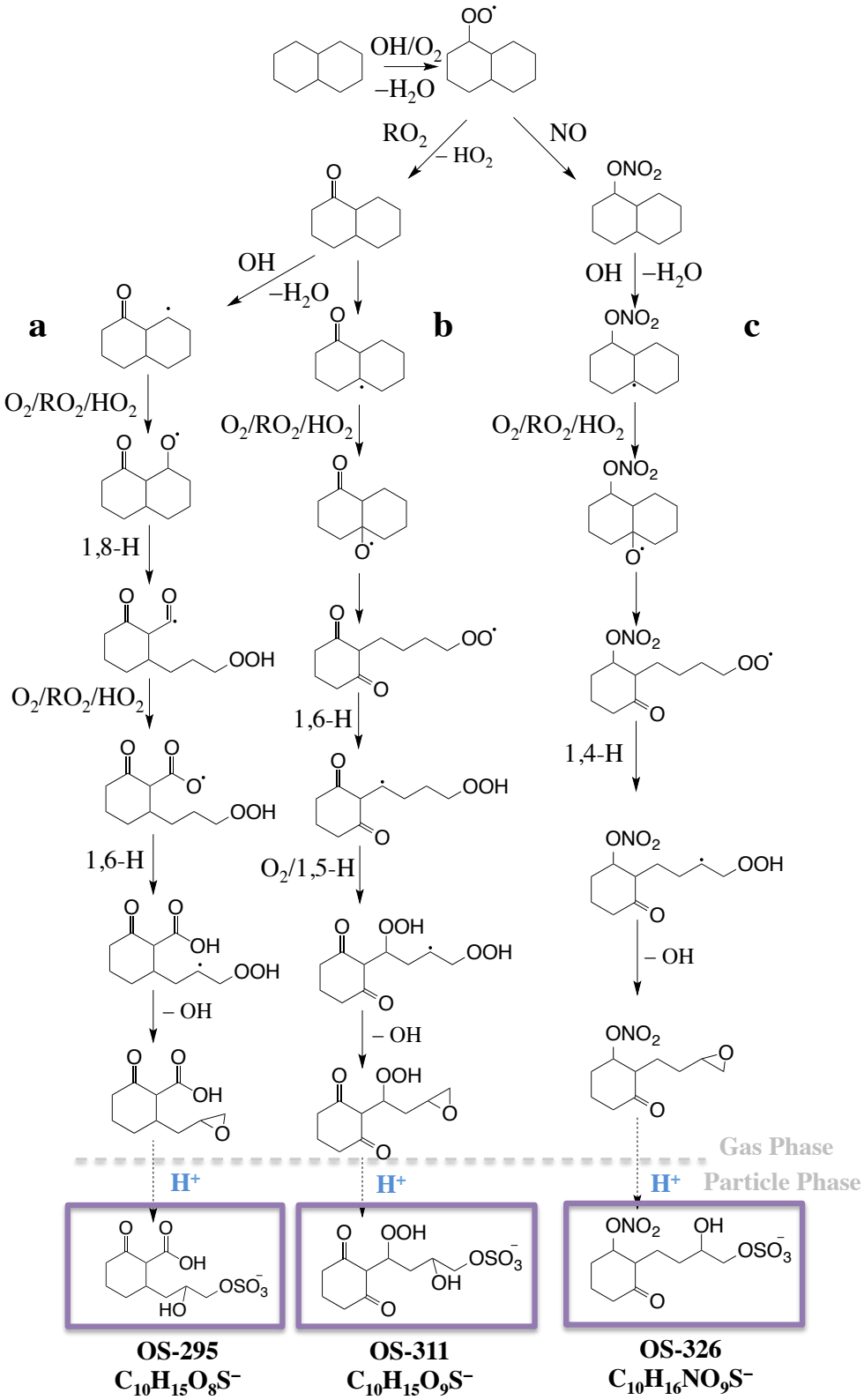

Figure 4. Tentatively proposed formation pathways of OS-295 (295.0494), OS-311 (*m/z* 311.0447) and OS-326 (326.0554) from the oxidation of decalin in the presence of sulfate aerosol.

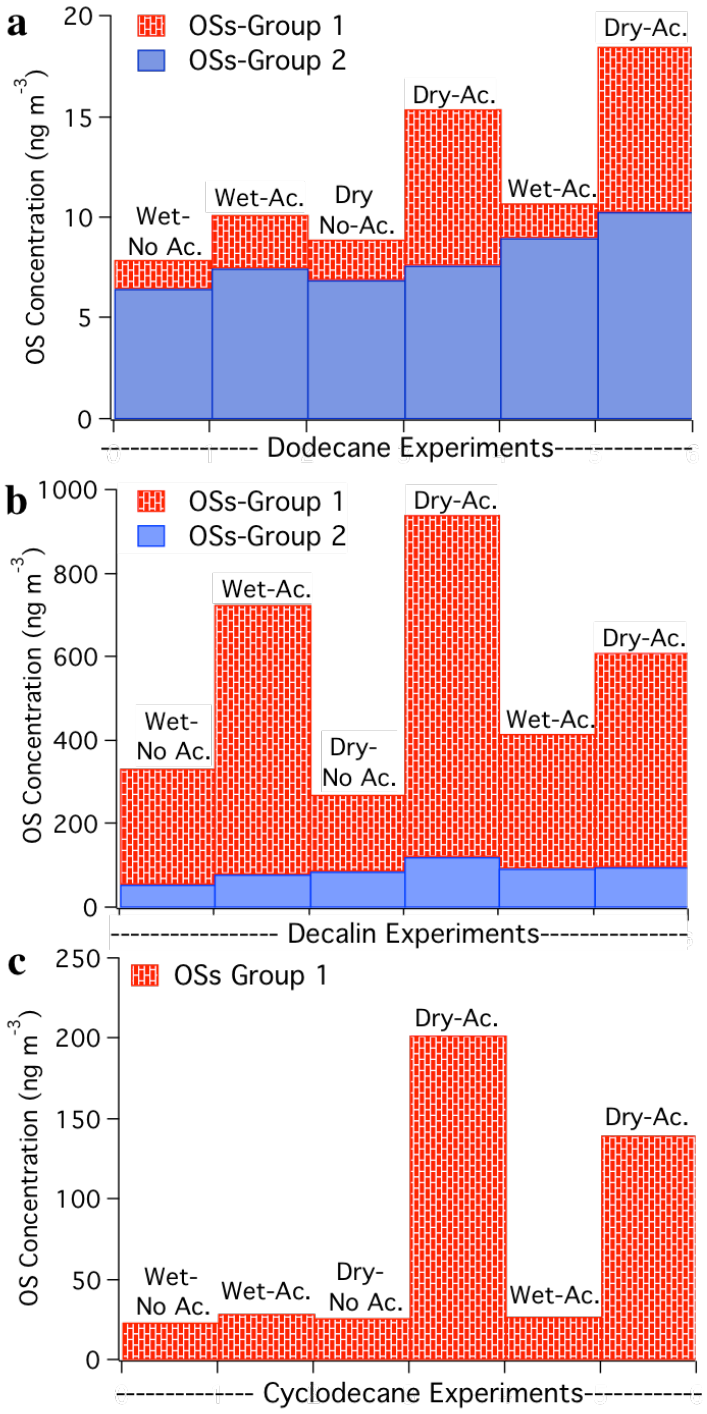

Figure 5. Impact of acidity on OS formation from gas-phase oxidation of (a) dodecane, (b) decalin, and (c) cyclodecane. OSs from Group-1 corresponds to compounds strongly impacted by aerosol acidity, while OSs from Group-2 appeared to have less dependency on aerosol acidity.

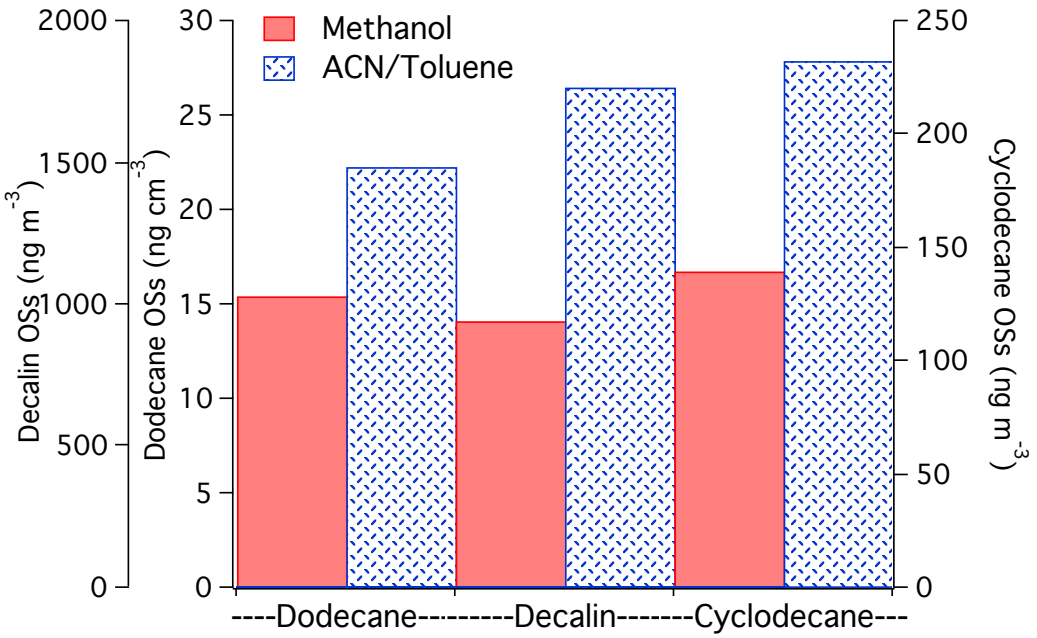

Figure 6. Impact of extraction solvent composition on quantification of identified OSs from gas-phase oxidation of alkanes.

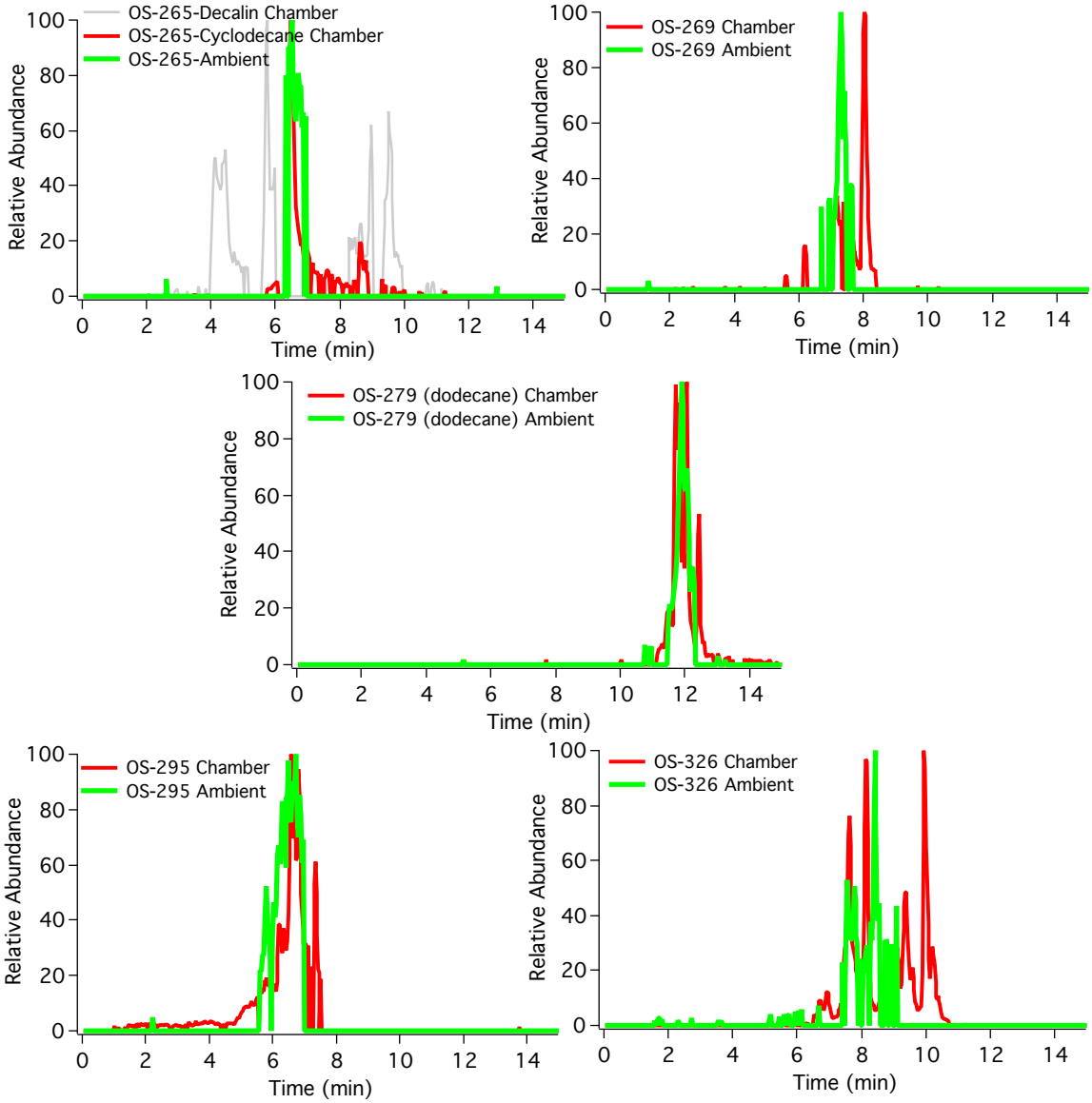

Figure 7. Extracted ion chromatograms (EICs) for selected alkane OSs identified in both smog chamber experiments (in red) and ambient samples (in green).